Wirkung von Propofol auf die Permeabilität in einem in-vitro-Modell der endothelialen Barriere der Blut-Hirn-Schranke und im Besonderen auf die Beeinflussung von oxidativem Stoffwechsel und Erkennung von DNA-Schäden auf Genomebene

Dissertation
zur Erlangung des akademischen Grades
Doktor der Medizin (Dr. med.)

vorgelegt
der Medizinischen Fakultät
der Martin-Luther-Universität Halle-Wittenberg

von Timo Längrich
geboren am in

Betreuer*innen: Prof. Dr. Rüdiger Horstkorte
apl. Prof. Dr. med. habil. Britt Hofmann

Gutachter*innen: Prof. Dr. Gábor Szabó, Halle (Saale)
Prof. Dr. Kerstin Danker, Berlin

Datum der Verteidigung: 22.10.2024

Referat

Aufgrund der besonderen Empfindlichkeit unseres Gehirns verfügt das Zentrale Nervensystem über eine hochspezialisierte Barriere, die Blut-Hirn-Schranke. Für deren Funktion spielt insbesondere die endotheliale Barriere und deren intensive Zell-Zell-Kontakte eine große Rolle. Störungen der Blut-Hirn-Schranke zeigen sich bei einer Vielzahl akuter und chronischer Erkrankungen. Eine Erkrankung, bei der die Blut-Hirn-Schranke eine wichtige Rolle zu spielen scheint, ist das postoperative Delir, welches eine häufige postoperative Komplikation besonders bei älteren Patienten darstellt. Dabei ist noch nicht klar, welche Rolle Anästhetika spielen. Insbesondere Propofol ist ein gut steuerbares und sehr weit verbreitetes Narkotikum, für das bereits verschiedene Nebenwirkungen auf molekularer Ebene beschrieben wurden.
Aus diesem Grund ist es Ziel dieser Arbeit, die Auswirkungen der Behandlung von humanen mikrovaskulären Endothelzellen mit Noradrenalin und Propofol zu untersuchen. Dazu wurde einerseits die Passagefähigkeit für das Bakterium E. coli bestimmt und andererseits mithilfe eines Fluorescein-Assays eine Permeabilitätsbestimmung für kleine Moleküle durchgeführt, jeweils in Abhängigkeit vom Vorhandensein von Noradrenalin oder Propofol. Dabei zeigte sich eine Permeabilitätserhöhung durch eine Behandlung mit Noradrenalin oder Propofol. Außerdem führte ich einen Zell-Adhäsions-Assay durch, bei dem sich keine deutlichen Unterschiede durch eine Propofol-Behandlung zeigten. Die Untersuchung von Veränderungen durch Propofol auf Genomebene wurden mittels Massenspektrometrie untersucht und gefundene Veränderungen im Western Blot verifiziert. Dabei zeigte sich keine verringerte Expression von Proteinen der Zell-Zell-Kontakte. Es zeigten sich andere Stoffwechselwege gestört, darunter der oxidative Metabolismus und *DNA damage recognition*. Insgesamt könnten die gefundenen Veränderungen erklären, wieso es zu einer erhöhten Permeabilität der Blut-Hirn-Schranke unter Propofol-Einfluss kommt. Zudem verdeutlicht es den möglichen Nutzen protektiver Substanzen zum Schutz vor einem postoperativen Delir.

Längrich, Timo: Wirkung von Propofol auf die Permeabilität in einem in-vitro-Modell der endothelialen Barriere der Blut-Hirn-Schranke und im Besonderen auf die Beeinflussung von oxidativem Stoffwechsel und Erkennung von DNA-Schäden auf Genomebene, Halle (Saale), Univ., Med. Fak., Diss., 61 Seiten, 2024

Inhaltsverzeichnis

Abkürzungen

AD	Alzheimer-Demenz
AGE	advanced glycation endproduct
AJ	adherens junction
ALS	Amyotrophe Lateralsklerose
BHS	Blut-Hirn-Schranke
BMEC(s)	brain microvascular endothelial cell(s)
CYP	Cytochrom P450
DDR	DNA damage response
EDTA	Ethylendiamin-tetraessigsäure
FTH1	Ferritin heavy chain
FTL	Ferritin light chain
GABA	γ-Aminobuttersäure
GLUT1	Solute carrier family 2, facilitated glucose transporter member 1
H2AX	Histon H2AX
ICU	Intensive care unit = Intensivstation
IL-1/ -6	Interleukin-1/ -6
iPSC	Induced pluripotent stem cells
MGO	Methylglyoxal
PECAM-1	platelet endothelial cell adhesion molecule-1
POD	Postoperatives Delir
PTM	posttranslationale Modifikation
ROS	reactive oxygen species
TIVA	Totale intravenöse Anästhesie
TJ	tight junction
TNF-α	Tumor-Nekrose-Faktor α
ZNS	Zentrales Nervensystem
ZO-1/2/3	Zonula occludens protein - 1/2/3

1. Einleitung und Zielstellung

1.1 Blut-Hirn-Schranke

1.1.1 Definition

Die Blut-Hirn-Schranke (BHS) bildet eine Barriere zwischen den Blutgefäßen und den Geweben des Zentralen Nervensystems (ZNS), also des Gehirns und des Rückenmarkes, und übt wichtige Funktionen bei der Homöostase aus. So verhindert sie das Übertreten von endogenen und exogenen Substanzen sowie Mikroorganismen aus dem Blut in das zentrale Nervensystem [4].

1.1.2 Aufbau

Die Blut-Hirn-Schranke setzt sich aus drei wesentlichen Zelltypen zusammen, welche miteinander interagieren und gemeinsam die Funktion der BHS sichern [5]. Diese sind die spezialisierten Endothelzellen der feinen Hirnkapillaren (*brain microvascular endothelial cells; BMECs)*, die Perizyten und die Astrozyten.

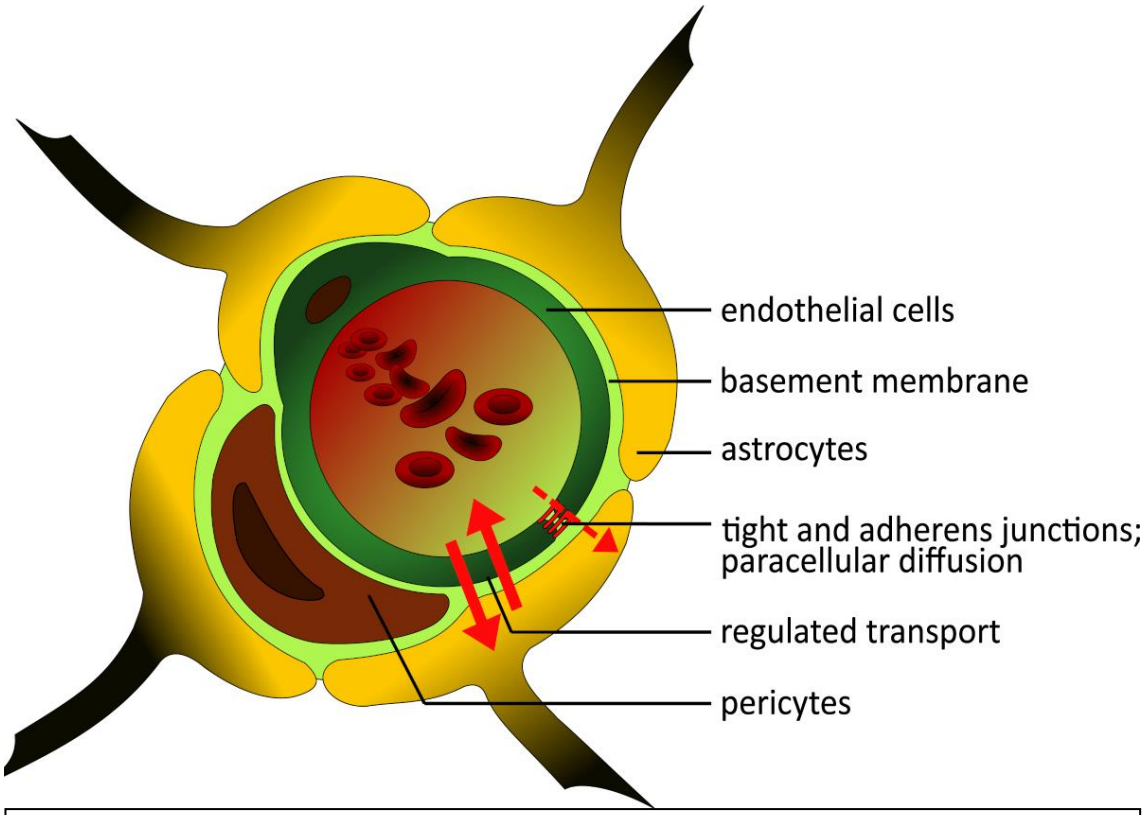

Abbildung 1: zelluläre Elemente der Blut-Hirn-Schranke und der Stoffaustausch

Quelle: Au - Weber, V., et al., Analyzing the Permeability of the Blood-Brain Barrier by Microbial Traversal through Microvascular Endothelial Cells. JoVE, 2020(156): p. e60692. [3]

1.1.2.1 Endothel

Das spezielle einschichtige Endothel der BHS unterscheidet sich deutlich von dem Endothel anderer Gewebe. So sitzen die BMECs einer kontinuierlichen Basalmembran auf und bilden zahlreiche *tight junctions* (TJ) und *adherens junctions* (AJ) untereinander aus, was den parazellulären Transport stark reduziert [6, 7]. Die Endothelzellen weisen zudem eine starke apikobasale Polarität auf, welche wichtig für den gerichteten und kontrollierten Stoffaustausch ist [8].

Eine wichtige Rolle für die Funktion der basal gelegenen AJ spielen dabei VE-Cadherin und PECAM-1. Diese regulieren vor allem die Migration von Leukozyten, genauso wie die Strukturproteine *endothelial cell-selective adhesion molecule* (ESAM) und *junctional adhesion molecule A/B/C* (JAM-A/-B/-C). Für die apikal gelegenen TJ ist die Expression von Occludin und Claudin-1, -3, -5 und -12, aber auch JAM-A, essenziell für die Regulation des parazellulären Transports von Ionen und löslichen Substanzen. So führt der Verlust von Claudinen bei neurodegenerativen Erkrankungen zu einer Störung der Barrierefunktion [9], während eine Induktion von Claudin-1 im Mausmodell die Passage von Tracerproteinen durch die BHS deutlich senkt [10]. Ebenso zeigt sich in der gestörten BHS bei Hirntumoren eine verringerte Expression von Occludin. Wichtig scheint auch die Verankerung der TJ-Proteine mit dem Zytoskelett über die Proteine ZO-1, -2 und -3 zu sein.

Für den selektiven transzellulären Transport sind die Endothelzellen mit zahlreichen spezifischen Transportproteinen ausgestattet [11-13] und weisen für die energieintensiven Transportvorgänge eine hohe Dichte an Mitochondrien auf [14]. Dies führt jedoch dazu, dass vermehrt reaktive ROS entstehen, die abgebaut werden müssen. So konnte gezeigt werden, dass ein gestörter Sauerstoff-Metabolismus und damit ein erhöhtes Auftreten von ROS eine Alzheimer-Demenz und Amyotrophe Lateralsklerose verschlechtern kann [15, 16].

1.1.2.2 Perizyten und Astrozyten

Die Perizyten, welche sich die Basallamina mit den Endothelzellen teilen und die Endothelzellen umgeben, unterstützen die Endothelzellen beim Aufbau einer Barriere, indem sie, unter anderem über die Ausschüttung von Retinsäure und *angiopoetin-1,* die Ausbildung von TJ sowie die Zusammensetzung der Basallamina beeinflussen [17-21]. Des Weiteren besitzen Perizyten die Fähigkeit, durch Phagozytose neurotoxische Substanzen zu eliminieren.

Es bestehen Interaktionen zwischen Perizyten und Astrozyten, unter anderem, indem eine synergistische Beeinflussung des Endothels und der neurovaskulären Kopplung erfolgt [18].

Astrozyten umgeben die Perizyten und bilden damit den Abschluss der BHS zum neuronalen Gewebe hin. Eine wichtige Rolle scheinen dabei die Perizyten bei der Expression von Aquaporin-4 (AQP-4) auf Astrozytenfüßchen zu spielen, während Astrozyten ihrerseits über Integrin α2 sowie Laminine Perizyten beeinflussen [22], aber auch Einfluss auf endotheliale TJ und AJ haben [23]. Eine Deletion der astrozytären *gap junction*-Proteine Connexin-43 und -30 führt zu einer Schwächung der Barrierefunktion vor allem gegenüber Leukozyten [24].

1.1.3 Funktion

Wie schon erwähnt erfüllt die Blut-Hirn-Schranke mehrere Aufgaben:

1.1.3.1 Barrierefunktion gegenüber Pathogenen und Neurotoxen

Im Blut befinden sich zahlreiche Stoffwechselprodukte, aber auch Noxen wie Medikamente und Toxine, auf die Neurone empfindlich reagieren. Ebenso besteht die Gefahr der Passage von Viren und Bakterien, die im Blut zirkulieren und eine (Meningo)-Enzephalitis auslösen können. Aus diesem Grund ist es notwendig, das ZNS vor ebensolchen Einflüssen zu schützen, was eine der Hauptaufgabe der BHS ist. So können nur wenige Substanzen, vor allem Gase und kleine lipophile Stoffe, die Blut-Hirn-Schranke penetrieren, während insbesondere geladene und damit hydrophile Moleküle nicht frei durch die Barriere diffundieren können, ebenso wenig wie Infektionserreger [25]. Eine wichtige Rolle spielen dabei Efflux-Systeme, die vom Endothel aufgenommene unerwünschte Substanzen wieder ins Blut zurück transportieren. Auf diese wird im Folgenden noch eingegangen.

Die regulatorische Funktion der Perizyten auf die Barrierefunktion scheint dabei ebenfalls essenziell zu sein, da eine Defizienz an Perizyten die Transzytose-Rate deutlich steigert [26].

Die Regulation der Transzytose und der TJ scheint jedoch unabhängig voneinander zu sein, da bei einem ischämischen Insult die frühe Öffnung der BHS vor allem auf der Erhöhung der Transzytose und nicht dem Kollaps der TJ basiert [27].

1.1.3.2 Transport von Molekülen zwischen Blut und ZNS

Die hohe Dichtigkeit der endothelialen Barriere stellt auch ein Hindernis für die Versorgung der Neurone dar, welche in hohem Maße auf die Verwertung von Glucose

angewiesen sind, gleichzeitig diese aber kaum speichern können. Glucose kann jedoch nicht frei durch die BHS diffundieren, sodass Transportproteine exprimiert werden müssen [28]. So ist das für den Glucosetransporter GLUT1 kodierende Gen SLC2A1 eines der meistkodierten im (murinen) BHS-Endothel [29]. Ebenso werden auch Aminosäuren, Ketonkörper, Hormone, Fettsäuren, Nukleotide und andere Substrate des Hirnstoffwechsels über Carrier transzellulär aus dem Blut in das Hirn transportiert. Für einzelne Substanzen, darunter Transferrin, Leptin und Triiodthyronin (T_3) existieren auch spezifische rezeptorvermittelte Transportwege über das Endothel [30]. Einige Viren, darunter das Varizella-Zoster-Virus (VZV) und HIV-1, können jedoch diese Transportproteine nutzen, um die endotheliale Barriere zu überwinden [31].

Umgekehrt existieren auch zahlreiche Transporter für nahezu alle Stoffklassen, die Stoffwechselendprodukte und Medikamente aus dem Hirninterstitium entfernen, darunter *ATP-dependent translocase* ABCB1 (P-Glykoprotein), *breast cancer resistance protein* (BCRP) und *multidrug resistance-associated proteins 1–5* (MRP1/2/3/4/5). So kann, vermittelt über die Proteine *Low Density Lipoprotein Receptor-related Protein 1* (LRP1), *phosphatidylinositol binding clathrin assembly protein* (PICALM) und Rab11 das Protein Aβ, dessen Ansammlung eine wichtige Rolle bei der Alzheimer-Demenz spielt, per Transzytose aus dem Hirn ins Blut geschleust werden [32]. Auf der anderen Seite scheint der *receptor for advanced glycation end products* (RAGE) im Mausmodell einen Transport von Aβ aus dem Blut ins Hirngewebe zu fördern, was zu Neuroinflammation führt [33]. Damit stellen diese Transportproteine auch wichtige Angriffspunkte für zukünftige Therapieoptionen dar.

Perizyten besitzen ebenfalls zahlreiche Transport-Proteine, die es ihnen ermöglichen, vor allem exzitatorische Aminosäuren aus dem ZNS zu eliminieren [26, 34].

1.1.3.3 Steuerung des zerebralen Blutflusses

Einzelne Subtypen von Perizyten scheinen in der Lage zu sein, sich zu kontrahieren und somit den mikrovaskulären Blutfluss, vor allem im Bereich der Arteriolen, zu regulieren [35]. Dazu exprimieren sie *α-smooth muscle actin* (α-SMA), Tropomyosin und Desmin. Die Steuerung der Vasodilation erfolgt bei erhöhten Neurotransmitter-Konzentrationen über die NO-abhängige Freisetzung von Prostaglandinen.

1.1.3.4 Aufrechterhaltung der zerebralen Homöstase

Für eine physiologische Funktion der Neurone des ZNS wird die Konstanthaltung eines spezifischen Milieus benötigt. Neurone reagieren empfindlich auf Veränderung des Milieus, zum Beispiel des pH-Wertes oder osmotische Veränderungen [36]. Sie weisen

eine hohe Aktivität der Na^+-K^+-ATPase auf, um die, für andere Transporter und ein stabiles Membranpotenzial notwendigen, hohen Natrium- und niedrigen Kalium-Spiegel aufrecht zu erhalten.

Infolge des mangelnden Regenerationspotenzials der Neurone müssen entzündliche Prozesse im Gehirn verhindert werden, weswegen auch die immunregulatorische Funktion gegenüber Zytokinen und Leukozyten essentiell ist [37]. So kommt es bei der Alzheimer-Demenz zu einer Migration von Monozyten in das ZNS; unter anderem vermittelt über PECAM-1 und RAGE.

Die Endothelzellen können nach Bindung von Lipopolysacchariden (LPS) aus dem Blut über die Sekretion von Prostaglandin E2 auch selbst Fieber auslösen [38].

1.1.4 Blut-Hirn-Schranke bei Erkrankungen

Einige neurodegenerative Erkrankungen, darunter die Alzheimer-Demenz, Morbus Parkinson und Amyotrophe Lateralsklerose gehen mit Veränderungen der BHS einher [36, 39], wobei nicht klar ist, ob die Veränderungen der BHS eine Ursache oder Folge der Erkrankungen sind. Bei der Amyotrophen Lateralsklerose scheint, neben dem Durchtritt von Molekülen aus dem Blut in das ZNS, auch eine Reduktion der Anzahl der Perizyten aufzutreten [40, 41]. Besonders entzündliche Zustände scheinen über die Zytokine TNF-α und IL-1β die Expression von zellulären Adhäsionsmolekülen zu fördern, was dann zur Bindung und Infiltration von Leukozyten führt [42-44].

Bei der septischen Enzephalopathie zeigt sich eine erhöhte Permeabilität für Eisen aufgrund einer veränderten Signaltransduktion mit Akkumulation von kolloidalem Eisen [45, 46]. Ebenso kommt es bei zerebraler Ischämie zu einer biphasischen Öffnung der BHS mit folgendem Hirnödem [47, 48]. Bei der Meningitis und Sepsis kommt es im Rahmen der entzündlichen Reaktion zudem zu einer erhöhten Permeabilität unter anderem für Albumin [49], dabei ist die Sepsis ebenfalls assoziiert mit einem postoperativen Delir [50].

1.2 Advanced Glycation Endproducts

Advanced Gylcation Endproducts (AGE) entstehen durch Glykierung, eine nicht-enzymatische Reaktion von reduzierenden Kohlenhydraten mit freien Aminogruppen von Proteinen. Während dieser Reaktion, der Maillard-Reaktion, bilden sich als Zwischenprodukte Schiff'sche Basen, welche sich zu Amadori-Produkten und schließlich AGE umlagern [51]. Da AGEs mit zunehmendem Alter im Körper

akkumulieren, werden sie auch als einer der molekularen Mechanismen zellulären Alterns aufgefasst [52, 53].

Während der Bildung von AGEs kann sich aus den Amadori-Produkten Methylglyoxal (MGO) bilden, ein Dicarbonyl, welches auch während der Glykolyse als Nebenprodukt entsteht [54, 55]. MGO ist selbst sehr reaktiv und wiederum in der Lage, AGEs zu bilden. MGO kann als Marker für Carbonylstress, wie er zum Beispiel bei Diabetes mellitus auftritt, angesehen werden.

Durch die veränderte Proteinstruktur und Kreuzvernetzungen wird die Funktion der Proteine bis zum kompletten Funktionsverlust gestört. Außerdem binden AGE an den *receptor for advanced glycation end products* (RAGE) und können darüber pro-inflammatorische Kaskaden auslösen [56]. Letztlich zeigen Endothelzellen, welche in glucosereichem Medium kultiviert wurden, eine erhöhte endotheliale Permeabilität sowie eine erhöhte RAGE-Aktivität [57].

1.3 Anästhetika

1.3.1 Propofol

Propofol gehört zu den am häufigsten gebrauchten Substanzen in der Anästhesie. Es findet als Injektionsnarkotikum breite Verwendung bei der Einleitung und Aufrechterhaltung einer Narkose sowie, wegen seiner kurzen Halbwertszeit, für die Analgosedierung. Da es im Gegensatz zu Inhalationsnarkotika keine Triggersubstanz für Maligne Hyperthermie darstellt und zudem seltener Postoperative Übelkeit und Erbrechen (PONV) hervorruft, kann es auch bei entsprechend prädispositionierten Patienten verwendet werden [58].

Chemisch handelt es sich bei Propofol um 2,6-Diisopropylphenol, eine Substanz, welche aufgrund ihrer ausgeprägten Lipophilie die BHS problemlos penetrieren kann. Die gleichzeitig resultierende schlechte Wasserlöslichkeit führt dazu, dass Propofol im klinischen Alltag in Sojaöl (100 mg/ml) gelöst und anschließend zusammen mit Glycerin (22,5 mg/ml) mittels Eilecithin (12 mg/ml) in Wasser emulgiert wird. Aufgrund dessen gilt laut Fachinformation Propofol bei Patienten mit Sojaallergie als kontraindiziert, wofür sich in Studien jedoch keine Evidenz findet [59]. Aufgrund des Lipidanteils ist die Zugabe von antimikrobiellen Substanzen wie EDTA nötig, um eine mikrobielle Kontamination mit septischer Folge zu vermeiden.

Als klinisch relevante Nebenwirkungen treten Injektionsschmerz, Träume, Blutdruckabfall und Atemdepression auf. Als seltene Nebenwirkung tritt bei

Dauerinfusion das lebensgefährliche Propofol-Infusionssyndrom mit Laktatazidose, Rhabdomyolyse und Nierenversagen auf. Möglicherweise sind die Effekte nicht auf Propofol selbst zurückzuführen, sondern auf die Zusatzstoffe, die für die Lösung und Stabilisierung notwendig sind [60].

Die Wirkungsweise von Propofol ist nicht genau verstanden. Aktuell wird vor allem die Bindung an inhibitorische $GABA_A$- und Glycin-Kanäle im Gehirn als Hauptwirkung angesehen [61], aber auch weitere mögliche molekulare Ziele wurden identifiziert. Durch Potenzierung der Rezeptorwirkung in bestimmten Hirnregionen, u.a. Thalamus und Formatio reticularis des Hirnstamms, erfolgt dann der hypnotische Effekt [62, 63].

Die Metabolisierung von Propofol findet fast ausschließlich in der Leber statt, wo Propofol größtenteils über UDP-Glucuronidierung inaktiviert und wasserlöslich gemacht wird und anschließend über die Nieren ausgeschieden wird [64]. Ein kleinerer Teil (ca. 29%) wird CYP-abhängig hydroxyliert, anschließend konjugiert und ebenfalls über die Niere ausgeschieden.

Die Auswirkungen von Propofol auf die Funktion der BHS sind umstritten. Zuletzt konnte gezeigt werden, dass Propofol oxidativen Stress nach renaler Ischämie reduzieren kann [65]. Außerdem scheint es kardioprotektiv bei Herzoperationen zu wirken, indem es die mitochondriale Funktion über die Regulation von Cytochrom C, Connexin 43 und mtDNA beeinflusst [66]. Bei der Verwendung bei koronarer Bypass-Chirurgie findet sich eine Reduktion der Schädigung des Myokards durch freie Radikale, der Lipid-Peroxidation sowie eine Reduktion der systemischen Entzündungsreaktion [67]. Es wird vermutet, dass diese Effekte auch zu einer Permeabilitätserhöhung der BHS führen könnten. Auf der anderen Seite zeigt sich in einem in-vitro-Modell durch Propofol eine Reduktion der durch eine 2%ige Hypoxie induzierten veränderten Permeabilität der BHS [68]. Zudem reduziert Propofol die ROS-Level, dadurch bedingte DNA-Strangbrüche und hemmt die Apoptose im Skelettmuskelzellmodell [69], gleichzeitig gibt es aber auch Hinweise auf eine Erhöhung von ROS-Leveln in humanen BMEC [70].

1.3.2 Noradrenalin

Noradrenalin (=Norepinephrin) ist selbst kein Anästhetikum, sondern ein, auch endogen vorkommendes, Katecholamin. Es findet zur Kreislaufstabilisierung breite Anwendung während einer Allgemeinanästhesie. Als peripher freigesetztes Hormon wirkt es vor allem über die Aktivierung von adrenergen α- und β_1-Rezeptoren [71] sowie als wesentlicher Transmitter des Sympathikus über vorgenannte Rezeptoren

sowie als Neurotransmitter im Gehirn. Im Zuge der Sympathikuswirkung führt es unter anderem zu Vasokonstriktion, Bronchodilatation, Tachykardie, Mydriasis und Hemmung der Magen-Darm-Peristaltik. Als Medikament verabreicht ist aufgrund der hohen Affinität zu α_1-Rezeptoren vor allem die Vasokonstriktion relevant [72]. Im ZNS fungiert Noradrenalin als Neurotransmitter im noradrenergen System, wobei die höchste Konzentration noradrenerger Neurone im Locus coeruleus zu finden ist. Das noradrenerge System spielt eine wichtige Rolle bei der Schlaf-Wach-Regulation, bei der Gedächtnisbildung und in der endogenen Schmerzhemmung [71]. Interessanterweise wurde auch vermutet, dass der Locus coerulus auch eine Rolle für eine mangelnde Permeabilität für Makromoleküle spielt [73].

In einem in-vitro-Modell führte die Applikation einer supraphysiologischen Konzentration von Noradrenalin zusammen mit Dobutamin und Adrenalin auf *immortalized murine microvascular endothelial cell[s] from the cerebral cortex* zu einer Veränderung der Zellmorphologie mit verminderter Expression von ZO-1, Claudin-5 und VE-Cadherin auf Protein- und mRNA-Ebene [74]. Besonders ausgeprägt zeigte sich dies im Zusammenspiel mit Reoxigenierung nach einer Phase von Hypoxie.

1.4 Postoperatives Delir

Das postoperative Delir, früher als Durchgangssyndrom bezeichnet, spielt eine große Rolle bei den passageren Komplikationen von Operationen bzw. der notwendigen Allgemeinanästhesien, besonders beim älteren Menschen. Ein Delir wird als vorübergehende fluktuierende Veränderung von Kognition und/oder Aufmerksamkeit definiert. Die Bandbreite der Symptome reicht von Desorientierheit, emotionaler Dysregulation, verminderter Aktivität bis zu Agitation und Halluzinationen. Bis zu 55% aller PatientInnen über 70 Jahren weisen nach einer kardiochirugischen Operation Symptome eines POD auf [75]. Allgemein tritt ein POD bei ca. 20% aller operierten Über-70-Jährigen auf [76]. Als Risikofaktoren wurden unter anderem Alter, Komorbiditäten (z.B. Diabetes mellitus), Dehydratation, intraoperative Blutung und postoperativer Schmerz identifiziert [77].

Zur Entstehung eines Delirs gibt es nach Maldonado vier wesentliche Faktoren, welche miteinander interagieren [78]:

1) neuronale Alterung
2) inflammatorische Reaktion
3) Glucocorticoiden als neuroendokrine Stressantwort
4) oxidativer Stress

Alle diese Faktoren scheinen über eine Störung der Neurotransmission zu einer Störung neuronaler Netzwerke mit Dysregulation der Schlaf-Wach-Rhythmik zu führen.

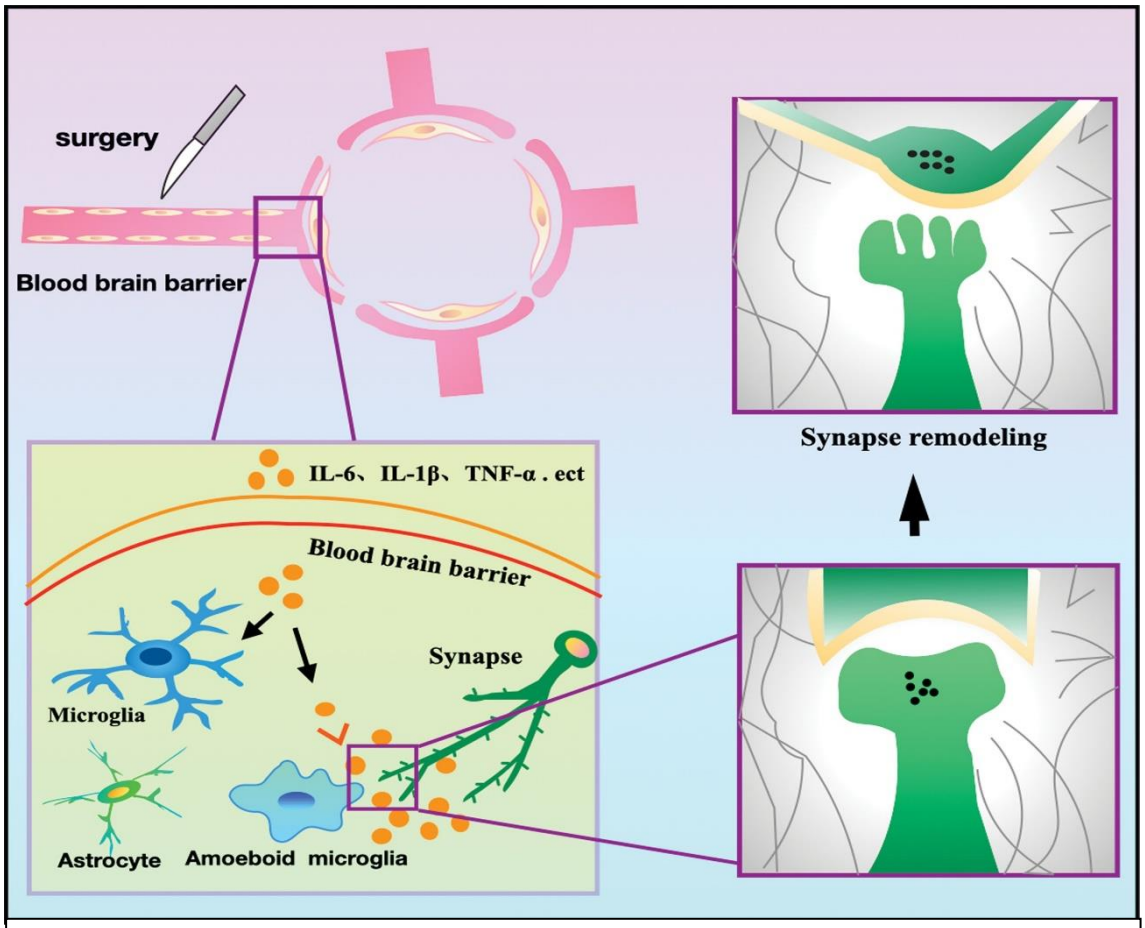

Abbildung 2: Neuroinflammation führt zu synaptischen Remodelling

Quelle: Xiao, M.Z., et al., Postoperative delirium, neuroinflammation, and influencing factors of postoperative delirium: A review. Medicine, 2023. ***102****(8): p. e32991. [2]*

Speziell bei der Entstehung eines POD scheint die Stress-Antwort auf den operativen Eingriff eine wichtige Rolle zu spielen. Über eine Aktivierung der Hypophysen-Nebennieren-Achse kommt es zur Freisetzung von Noradrenalin, Adrenalin und Cortisol. Eigentlich sind alle gängigen Anästhetika Hemmstoffe dieser Antwort auf intraoperativen Stress. So kommt es zu einer Hemmung der Aktivierung der sympathischen Antwort mit einer verringerten Ausschüttung von Noradrenalin, Adrenalin und Cortisol. Bei Propofol ist dieser Effekt teilweise sogar stärker ausgeprägt als bei volatilen Anästhetika [79, 80]. Trotzdem zeigt sich keine verringerte Rate an POD in einer Propofol-haltigen TIVA im Vergleich zu einer Anästhesie mit Sevofluran [81]. Außerdem wurde bei Ratten gezeigt, dass volatile Anästhetika zu einer

Veränderung und Permeabilitätserhöhung der BHS für Immunglobin G führen, vor allem bei gealterten Ratten, was eine Beziehung zum POD vermuten lässt [82].

Erhöhte Serumkonzentrationen von Noradrenalin zeigen eine Assoziation sowohl mit einem *ICU-aquired delirium* als auch einem POD, allerdings nur bei Patienten, die keine Katecholamin-Behandlung erhielten. Das spricht dafür, dass die Noradrenalin-Spiegel nur Ausdruck eines erhöhten Sympathikotonus sind und Noradrenalin nicht selbst delirogen ist [83].

Insgesamt scheint besonders das gealterte ZNS schlechter auf den perioperativen Stress reagieren zu können, was dann zu Störungen führt. Die Freisetzung von Entzündungsmediatoren wie IL-1, IL-6 und TNF-α im Zuge einer Operation führt unter anderem zu einer endothelialen Dysfunktion, mit einer Reduktion von TJ-Proteinen wie Occludin und ZO-1 im Mausmodell [84].

Dies wiederum führt zu einer Migration von Monozyten und Mastzellen ins Hirnparenchym und es kommt zu einer Aktivierung von Mikroglia und Astrozyten. Eine Rolle bei dieser Aktivierung spielen Proteine, die als *danger-associated molecular patterns* (DAMPs) agieren, wie S100A8 und *high-mobility group box 1 protein* (HMGB-1) [85, 86]. Von der folgenden Neuroinflammation mit neuronaler Schädigung und Apoptose scheint besonders auch der Hippocampus betroffen zu sein [87]. Insgesamt führt diese Neuroinflammation zur synaptischen Dysfunktion und zu neuronaler Apoptose [88].

Im Mausmodell zeigt sich eine Senkung des Auftretens von postoperativen kognitiven Einschränkungen durch den Einsatz des Eisen-Chelators Deferoxamin, was dafür spricht, dass auch eine Störung der Eisen-Homöstase Teil der Pathophysiologie des POD sein könnte [89]

Die Aktivierung von cholinergen Signalwegen über den vagalen Reflex kann eine überschießende inflammatorische Reaktion durch eine Suppression von IL-1β und TNF-α regulieren [90]. Deshalb könnte eine verminderte Aktivität des cholinergen Neurotransmittersystems mit einem (postoperativen) Delir assoziiert sein [91, 92], was auch erklärt, warum anticholinerg wirkende Medikamente ein delirogenes Potenzial besitzen.

Besonders wichtig für die Entstehung eines POD scheint aber auch ein gealtertes ZNS mit einer gealterten BHS zu sein. Vermutlich reichen dann die funktionellen anti-inflammatorischen Reserven nicht aus und es kommt zu einer gesteigerten inflammatorischen Reaktion [93].

1.5 Zielstellung

Die Integrität der BHS zeigt sich bei zahlreichen chronischen und akuten Erkrankungen gestört. Besonders bei den Krankheitsbildern der Sepsis und des postoperativen Delirs spielt möglicherweise eine Störung der Barrierefunktion eine wesentliche Rolle. Dazu ist es nötig, zu verstehen, was diese Störungen auslösen kann und ob dabei Prozesse des Alterns, zum Beispiel in Form der Bildung von AGE, oder bestimmte Medikamente eine Rolle spielen. Diese Faktoren und ihre Wirkungsweise zu identifizieren, ermöglicht es, gegebenenfalls präventive Maßnahmen zu ergreifen oder bestimmte Auslöser zu meiden.

Ziel der Arbeit ist es, mit Hilfe eines zuvor etablierten in-vitro-Modells der endothelialen Barriere der BHS, die Auswirkungen der Bildung von AGE auf die Dichtigkeit der Barriere zu untersuchen. Dazu wird nach einer Behandlung der Endothelzellen mit MGO die Bildung von AGE induziert. Daraufhin kann die Fähigkeit der Passage von E. coli mit und ohne AGE-Induktion verglichen werden, genauso wie unter Einwirkung von zwei typischen Medikamenten der Allgemeinanästhesie: Propofol und Noradrenalin. Um eine Prüfung der Reversibilität der AGE-induzierten Effekte durch die antioxidative Substanz Ascorbinsäure (Vitamin C) zu prüfen, erfolgt zudem eine entsprechende Nachbehandlung.

Anschließend sollen die intrazellulären Effekte von Propofol genauer analysiert werden. Dazu erfolgt zunächst mittels Fluorescein-Assay eine Untersuchung der Permeabilität nach Propofol-Behandlung. Daran schließt sich eine massenspektrometrische Analyse des Proteoms verschieden behandelter Endothelzellen an. Dies dient der Suche nach relevanten Veränderungen der Proteinexpression unter dem Einfluss von Propofol. Anhand dessen sollen Proteingruppen und Stoffwechselwege identifiziert werden, die besonders beeinflusst werden. Schlussendlich erfolgt eine Bestätigung der Ergebnisse der Massenspektrometrie mittels Western Blots für ausgewählte Proteine. Bei allen Untersuchungen erfolgt immer auch ein Vergleich mit der Trägerlösung für Propofol, um Effekte dieser lipidhaltigen Lösung ausschließen zu können.

2. Diskussion

2.1 Glykierung des Endothels führt zu erhöhter Permeabilität

Wie erwartet führt die Behandlung von Endothelzellen mit MGO zur Glykierung von Proteinen der Endothelzellen. Bereits eine Konzentration, die auch im menschlichen Organismus gemessen werden kann, erhöht allerdings auch die Permeabilität für Escherichia coli, was für eine Störung der trans- oder parazellulären Barrierefunktion spricht, sodass die Bakterien leichter die Barriere passieren können. Gleichzeitig sinkt die Viabilität der Zellen nicht, das heißt, die Barrierestörung ist nicht auf eine Zelltoxizität zurückzuführen. Dicarbonylstress führt also dazu, dass die endotheliale Barriere gestört wird, was auch durch andere Veröffentlichungen bestätigt wird [94-96]. Auch in klinischen Studien zeigt sich für Diabetes mellitus, welcher über die erhöhten Blutglucosekonzentrationen zu einer Belastung mit Dicarbonylen führt, eine Korrelation mit dem vermehrten Auftreten von Meningitis [97, 98] und POD [75].

2.2 AGE verstärken Effekte von Noradrenalin und Propofol auf die Permeabilität

Propofol findet als Hypnotikum breite Verwendung bei der Allgemeinanästhesie, genauso wie Noradrenalin zur Kreislaufstabilisierung sowohl während der OP als auch in der Intensivmedizin.

Bei einer Konzentration von Propofol, die der entspricht, welche auch klinisch angewendet wird, zeigt sich eine erhöhte Permeabilität für E. coli, ähnlich wie bei der alleinigen Induktion von Glykierung durch MGO. Klinisch könnte eine solche Bakterienmigration eine Meningitis auslösen. Genauso wie für Bakterien steigt wahrscheinlich auch die Permeabilität für kleinere Stoffe (siehe auch 2.4.), die wiederum verantwortlich für ein POD sein können. Insgesamt können also schädigende Effekte von Propofol auf das Endothel angenommen werden, wie auch schon andere Arbeiten vermuten [99, 100]. Für eine Behandlung mit Noradrenalin zeigt sich genauso eine erhöhte Permeabilität für E. coli. Klinisch lässt sich aber kein Zusammenhang zwischen Noradrenalinspiegel und POD finden [101].

Es zeigt sich ein additiver Effekt bei MGO-Vorbehandlung, welche Effekte der erhöhten Glucosekonzentration bei Diabetes mellitus imitieren soll. Dies wiederum passt zu klinischen Beobachtungen, welche eine erhöhte Inzidenz für POD bei Diabetikern

zeigen [75]. Umso wichtiger scheint auch die prä- und intraoperative Normoglykämie zu sein, da Hyperglykämie mit vermehrtem Auftreten von POD assoziiert ist [102].

2.3 Ascorbinsäure hat protektive Effekte auf die Permeabilitätserhöhung durch AGE

Ascorbinsäure, allgemein bekannt als Vitamin C, ist eine reduzierende bzw. antioxidative Substanz und damit in der Lage Glykierung zu verhindern, zum Beispiel bei Hämoglobin [103]. Dadurch stellt sich die Frage, ob Ascorbinsäure in der Lage ist, die Effekte der Glykierung durch MGO zu neutralisieren. Tatsächlich zeigt sich eine partielle Reversibilität durch die Applikation von Ascorbinsäure mit verringertem Durchtritt von Bakterien. Ascorbinsäure kann über die Eliminierung von freien Radikalen eine Hemmung der systemischen Entzündungsreaktion bewirken [104]. Besonders postoperative Patienten weisen stark erhöhte Mengen an ROS auf, welche die antioxidativen Kapazitäten regelmäßig übersteigen [105]. Dies führt zur vermehrten Bildung von AGEs, mit einer folgenden Schädigung von Proteinen, auch der BHS, was schließlich zu einem POD führen kann. Hier könnte Ascorbinsäure antioxidative Funktionen übernehmen. Da die verwendete Konzentration auch im klinischen Alltag erreicht werden, ist es möglich, dass die (perioperative) Applikation von Ascorbinsäure ein postoperatives Delir verhindern könnte. Dies muss in vivo untersucht werden. Besonders hohe ROS-Konzentrationen werden dabei bei Hyperglykämie, vor allem bei Diabetes mellitus, erreicht [106], weshalb gerade Diabetiker besonders von einer Hemmung der Bildung von AGE durch Ascorbinsäure [107] profitieren könnten.

2.4 Permeabilität für kleine Moleküle steigt durch Propofol-Einfluss

Es ist nicht klar, auf welchen Wegen E. coli die endotheliale Barriere passieren kann, ob dies auf transzellulärem oder parazellulärem Wege passiert. Wir konnten zeigen, dass die Passage nicht nur auf einer verminderten Resistenz gegenüber aktiven Passageversuchen der Bakterien beruht. Auch in einer Untersuchung mit Fluorescein zeigte sich eine erhöhte Permeabilität für dieses kleine Molekül, ähnlich wie es auch [108] beschreibt. Fluorescein ist ein Triphenylmethan-Farbstoff mit einem Molekulargewicht von 332 g/mol und kann als Modell für die Passage eines kleinen Moleküls dienen. Auch in Experimenten mit Ratten konnte bereits in vivo ein vermehrter Übertritt von Fluorescein ins ZNS nach einer traumatischen Hirnverletzung nachgewiesen werden [109].

2.5 Propofol beeinflusst über H2AX die Erkennung von DNA-Schäden

Das Histon-Protein H2AX ist eine Variante der Histon-H2A-Familie und somit Bestandteil der Nukleosomen. Besondere Bedeutung hat die phosphorylierte Form von H2AX, welche eine Rolle bei der Reparatur von DNA-Schäden (DDR) spielt und als Marker für DNA-Schäden fungieren kann [110]. Das phosphorylierte H2AX interagiert dabei mit Proteinen wie *Breast Cancer 1* (BRCA1) oder *Mediator of DNA damage checkpoint protein 1* (MDC1) und beeinflusst die Transkription von Genen, die über FoxO3a reguliert werden. Dadurch ist es assoziiert mit genomischer Stabilität und Langlebigkeit [111]. Deshalb könnte eine Herunterregulation von H2AX durch Propofol, wie sie sich in der Massenspektrometrie nachweisen ließ, auf längere Sicht Effekte zeigen, die zur beobachteten Störung des Endothels und damit der BHS führen. Insbesondere sind auch ROS und DDR eng miteinander verknüpft, weshalb man annehmen kann, dass eine Kombination beider Einflüsse, wie bei erhöhter Glucosebelastung und gleichzeitiger Propofol-Behandlung, die Zellen stark belastet und langfristig Apoptose induziert. Vor allem für Neurone zeigten sich schon hemmende Effekte auf Entwicklung [112] und Langzeitpotenzierung durch Propofol [113], was schließlich zu kognitiven Störungen führen kann. Deshalb könnte es gerade bei vorbelasteten Patienten, z.B. mit vorbestehendem Diabetes mellitus, hilfreich sein, antioxidative Substanzen wie Ascorbinsäure prophylaktisch einzusetzen. Somit wäre es klinisch vorstellbar, entsprechende Substanzen perioperativ zu verabreichen, um eine Schädigung durch Propofol und folgendem POD zu verhindern.

2.6 Propofol beeinflusst den Eisenstoffwechsel über eine Erhöhung von Ferritin und kann so langfristige Effekte auf die Funktion der BHS haben

Ferritin ist ein eisenbindendes Protein und als solches ein wichtiger Transporter in der BHS. Es besteht aus 24 Untereinheiten, welche zwei Isoformen aufweisen: *ferritin heavy chain* (FTH1) und *ferritin light chain* (FTL). Das Verhältnis von FTH1 und FTL ist dabei vom Gewebe abhängig, so zeigt sich in Herz und Gehirn eine höhere Konzentration von FTH1 [114]. Eine erhöhte Menge an Ferritin, wie sie unter Propofol-Einwirkung beobachtet wurde, könnte mit erhöhten Eisenkonzentrationen im ZNS verbunden sein. Langfristig führen Eisenansammlungen zu Folgeerkrankungen. Eisenansammlungen im ZNS sind mit Altern assoziiert und führen zu neuronalen Schäden durch Apoptose [115].

Zudem zeigt sich bei neurodegenerativen Erkrankungen eine Erhöhung des Verhältnisses von FTH1 zu FTL, wobei dies auf einen erhöhten Eisenumsatz mit Akkumulation hindeutet [116]. Folglich könnte Propofol über eine Eisenakkumulation eine Rolle spielen bei der Entstehung von Funktionsstörungen mit klinisch sichtbaren kognitiven Beeinträchtigungen. Dies erfordert eine kritischere Beurteilung des Einsatzes von Propofol als Anästhetikum und gegebenenfalls die Erforschung und den Einsatz protektiver Maßnahmen.

2.7 Propofol hat keine Auswirkungen auf die Expression von Zell-Zell-Kontakten

Aufgrund der Erhöhung der Permeabilität sowohl für Bakterien als auch für Fluorescein, ließe sich vermuten, dass durch Propofol-Einwirkung essenzielle Zell-Zell-Kontakte gestört werden. Ich konnte keine Zell-Adhäsions-Proteine finden, die signifikant hoch-/herunterreguliert wurden, was dafürspricht, dass deren Menge unter einer Propofol-Behandlung kaum verändert ist. Zwar ließen sich nur kurzfristige Effekte untersuchen, in diesem Zeitraum scheinen aber indirekte Effekte für die Permeabilitätserhöhung verantwortlich zu sein. Auf lange Sicht könnten diese Veränderungen aber eine entscheidende Rolle spielen. So zeigen ROS, welche auch vermehrt bei Diabetes mellitus auftreten, direkte schädigende Wirkungen auf Claudine, welche integrale Bestandteile von TJ sind [117]. Auch wäre es möglich, dass nicht die Quantität, sondern die intrazelluläre Lokalisation der Proteine der Zell-Zell-Kontakte verändert wird. Dazu fanden Hughes et al. eine veränderte Lokalisation, aber auch Expression von Occludin, nicht aber von ZO-1 und Claudin-5, unter Einfluss von Propofol [108]. Eine signifikante Rolle scheint nach deren Aussage die Matrix-Metalloprotease MMP-2 zu spielen.

2.8 Propofol und die posttranslationalen Modifikationen

Eine Rolle dabei können posttranslationale Modifikationen (PTM) spielen, was ich mit meiner Untersuchung nicht ausschließen kann. Unter anderem scheinen Phosphorylierung [118], Ubiquitinierung [119] und Palmitoylierung [120] eine Rolle für die Funktion der Zell-Adhäsions-Proteine zu spielen. In anderen Untersuchungen konnte gezeigt werden konnte, dass PTM die Funktion der BHS beeinflussen können [121]. Möglicherweise spielen gerade PTM eine Schlüsselrolle für die Funktion bzw. den Funktionsverlust unter Propofol-Einfluss.

Da die Phosphorylierung insbesondere für die Funktion von H2AX eine wichtige Rolle spielt, ist es sinnvoll, in einem Folgeexperiment zu untersuchen, ob sich neben der Expression auch die Phosphorylierung durch Propofol-Einfluss ändert.

Bei FTH1 zeigte sich, dass das Molekulargewicht unter Propofolbehandlung leicht ansteigt, was auf eine Phosphorylierung an zwei in der Literatur beschriebenen Serinen [122, 123] hindeuten kann, zusätzlich zur schon beschriebenen Hochregulation von FTH1.

2.9 Stärken und Limitationen

Ich konnte zum ersten Mal mittels Massenspektroskopie die Veränderungen auf Proteom-Ebene durch Propofol nachweisen und molekularbiologisch bestätigen. Damit ergeben sich Erklärungsansätze für die klinisch beschriebenen Funktionsstörungen durch Propofol und dessen mögliche Rolle bei der Entstehung des POD. Durch die Verwendung einer äquivalenten Lipidlösung als Kontrolllösung konnten zudem spezifisch die Effekte des Propofols untersucht werden.

Mittels des bereits etablierten in-vitro-Modells wird es zukünftig möglich sein, auch andere Substanzen auf ihre negativen Wirkungen auf BMECs zu untersuchen, genauso wie mögliche protektive Effekte. Es handelt sich jedoch um ein in-vitro-Modell, eventuelle Veränderungen müssen nicht zwangsläufig später auch in vivo nachweisbar sein.

Wie schon erwähnt konnte ich mit meinem Modell nicht prüfen, welche Rolle eine veränderte Lokalisation der Proteine der Zell-Zell-Kontakte spielt. Ich konnte zeigen, dass es zu keinen relevanten Veränderungen in der exprimierten Menge an Proteinen der Zell-Zell-Kontakte kommt. Eine eventuelle Lokalisationsänderung kann man in Folgeexperimenten mittels Fluoreszenzmikroskopie untersuchen, wie bei [108] geschehen. Allerdings nutzten hier die Autoren Endothelzellen, die aus iPSC differenziert wurden.

Auch können mit dem von mir verwendeten Modell nur Endothelzellen auf einer Basalmembran untersucht werden, die Interaktion mit Astrozyten und Perizyten kann nicht untersucht werden. Dies würde sich mit einem Modell darstellen lassen, bei dem eine Cokultur von Endothelzellen und Astrozyten und/oder Perizyten stattfindet.

2.10 Zusammenfassung

Zusammenfassend lässt sich sagen, dass die Glykierung von BMEC in-vitro zu einer Erhöhung der Permeabilität der endothelialen Barriere führt. Ascorbinsäure als reduzierende Substanz kann die Zellen vor Glykierung schützen und somit einer Permeabilitätserhöhung vorbeugen, beziehungsweise diese abmindern. Auch die Medikamente Noradrenalin und Propofol steigern die Permeabilität für Bakterien, insbesondere in Kombination mit Glykierung. Speziell für Propofol konnte ich zudem zeigen, dass auch kleine Moleküle die BHS besser passieren können. Dies beruht nicht auf einer Veränderung der Zellviabilität oder der veränderten Expression von Zell-Zell-Kontakten, sondern auf Veränderungen im Eisenstoffwechsel und der DNA-Schadens-Erkennung. Eine Rolle könnten auch posttranslationelle Modifikationen an H2AX spielen.

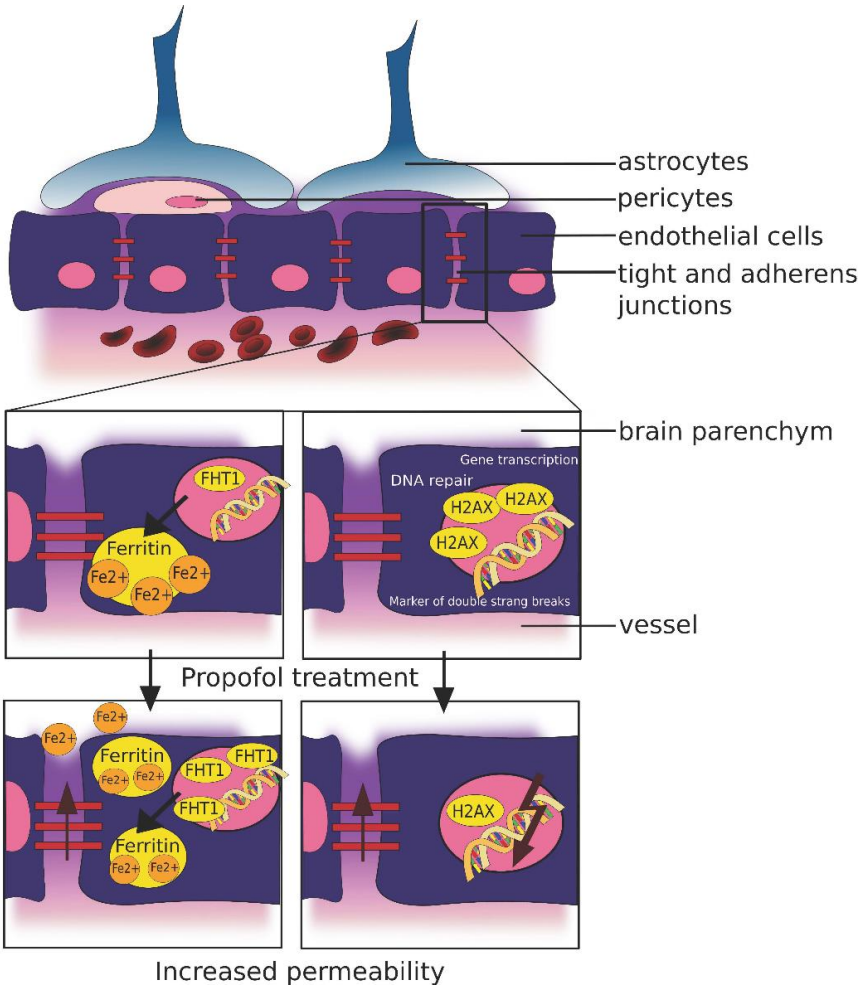

Abbildung 3: Propofol führt zu Störungen des Eisenstoffwechsels und der Erkennung von DNA-Schäden

Quelle: Längrich, T., et al., Disturbance of Key Cellular Subproteomes upon Propofol Treatment Is Associated with Increased Permeability of the Blood-Brain Barrier. Proteomes, 2022. 10(3): p. 28. [1]

3. Literaturverzeichnis

1. Längrich, T., et al., Disturbance of Key Cellular Subproteomes upon Propofol Treatment Is Associated with Increased Permeability of the Blood-Brain Barrier. Proteomes, 2022. **10**(3): p. 28.
2. Xiao, M.Z., et al., Postoperative delirium, neuroinflammation, and influencing factors of postoperative delirium: A review. Medicine, 2023. **102**(8): p. e32991.
3. Au - Weber, V., et al., Analyzing the Permeability of the Blood-Brain Barrier by Microbial Traversal through Microvascular Endothelial Cells. JoVE, 2020(156): p. e60692.
4. Montagne, A., Z. Zhao, and B.V. Zlokovic, Alzheimer's disease: A matter of blood-brain barrier dysfunction? J Exp Med, 2017. **214**(11): p. 3151-3169.
5. Ballabh, P., A. Braun, and M. Nedergaard, The blood-brain barrier: an overview: structure, regulation, and clinical implications. Neurobiol Dis, 2004. **16**(1): p. 1-13.
6. Brightman, M.W. and T.S. Reese, Junctions between intimately apposed cell membranes in the vertebrate brain. J Cell Biol, 1969. **40**(3): p. 648-77.
7. Morris, A.W., et al., Vascular basement membranes as pathways for the passage of fluid into and out of the brain. Acta Neuropathol, 2016. **131**(5): p. 725-36.
8. Worzfeld, T. and M. Schwaninger, Apicobasal polarity of brain endothelial cells. J Cereb Blood Flow Metab, 2016. **36**(2): p. 340-62.
9. Zlokovic, B.V., The blood-brain barrier in health and chronic neurodegenerative disorders. Neuron, 2008. **57**(2): p. 178-201.
10. Pfeiffer, F., et al., Claudin-1 induced sealing of blood-brain barrier tight junctions ameliorates chronic experimental autoimmune encephalomyelitis. Acta Neuropathol, 2011. **122**(5): p. 601-14.
11. Betz, A.L., J.A. Firth, and G.W. Goldstein, Polarity of the blood-brain barrier: distribution of enzymes between the luminal and antiluminal membranes of brain capillary endothelial cells. Brain Res, 1980. **192**(1): p. 17-28.
12. Betz, A.L. and G.W. Goldstein, Polarity of the blood-brain barrier: neutral amino acid transport into isolated brain capillaries. Science, 1978. **202**(4364): p. 225-7.
13. Mittapalli, R.K., et al., Exploiting nutrient transporters at the blood-brain barrier to improve brain distribution of small molecules. Ther Deliv, 2010. **1**(6): p. 775-84.
14. Oldendorf, W.H., M.E. Cornford, and W.J. Brown, The large apparent work capability of the blood-brain barrier: a study of the mitochondrial content of capillary endothelial cells in brain and other tissues of the rat. Ann Neurol, 1977. **1**(5): p. 409-17.
15. Palmer, A.M., The role of the blood-CNS barrier in CNS disorders and their treatment. Neurobiol Dis, 2010. **37**(1): p. 3-12.
16. Evans, M.C., et al., Inflammation and neurovascular changes in amyotrophic lateral sclerosis. Molecular and Cellular Neuroscience, 2013. **53**: p. 34-41.
17. Allt, G. and J.G. Lawrenson, Pericytes: cell biology and pathology. Cells Tissues Organs, 2001. **169**(1): p. 1-11.

18. Cai, W., et al., Pericytes in Brain Injury and Repair After Ischemic Stroke. Transl Stroke Res, 2017. **8**(2): p. 107-121.

19. Diaz-Flores, L., et al., Pericytes. Morphofunction, interactions and pathology in a quiescent and activated mesenchymal cell niche. Histol Histopathol, 2009. **24**(7): p. 909-69.

20. ElAli, A., P. Theriault, and S. Rivest, The role of pericytes in neurovascular unit remodeling in brain disorders. Int J Mol Sci, 2014. **15**(4): p. 6453-74.

21. Kim, J.H., et al., Recruitment of pericytes and astrocytes is closely related to the formation of tight junction in developing retinal vessels. J Neurosci Res, 2009. **87**(3): p. 653-9.

22. Yao, Y., et al., Astrocytic laminin regulates pericyte differentiation and maintains blood brain barrier integrity. Nat Commun, 2014. **5**: p. 3413.

23. Menezes, M.J., et al., The extracellular matrix protein laminin α2 regulates the maturation and function of the blood-brain barrier. J Neurosci, 2014. **34**(46): p. 15260-80.

24. Ezan, P., et al., Deletion of astroglial connexins weakens the blood-brain barrier. J Cereb Blood Flow Metab, 2012. **32**(8): p. 1457-67.

25. Juillerat-Jeanneret, L., The targeted delivery of cancer drugs across the blood-brain barrier: chemical modifications of drugs or drug-nanoparticles? Drug Discov Today, 2008. **13**(23-24): p. 1099-106.

26. Armulik, A., et al., Pericytes regulate the blood-brain barrier. Nature, 2010. **468**(7323): p. 557-61.

27. Knowland, D., et al., Stepwise recruitment of transcellular and paracellular pathways underlies blood-brain barrier breakdown in stroke. Neuron, 2014. **82**(3): p. 603-17.

28. Iadecola, C., The Neurovascular Unit Coming of Age: A Journey through Neurovascular Coupling in Health and Disease. Neuron, 2017. **96**(1): p. 17-42.

29. Daneman, R., et al., The mouse blood-brain barrier transcriptome: a new resource for understanding the development and function of brain endothelial cells. PLoS One, 2010. **5**(10): p. e13741.

30. Roberts, R.L., R.E. Fine, and A. Sandra, Receptor-mediated endocytosis of transferrin at the blood-brain barrier. J Cell Sci, 1993. **104 (Pt 2)**: p. 521-32.

31. Dohgu, S., et al., Human Immunodeficiency Virus-1 Uses the Mannose-6-Phosphate Receptor to Cross the Blood-Brain Barrier. PLOS ONE, 2012. **7**(6): p. e39565.

32. Zhao, Z., et al., Central role for PICALM in amyloid-β blood-brain barrier transcytosis and clearance. Nat Neurosci, 2015. **18**(7): p. 978-87.

33. Deane, R., et al., A multimodal RAGE-specific inhibitor reduces amyloid β-mediated brain disorder in a mouse model of Alzheimer disease. J Clin Invest, 2012. **122**(4): p. 1377-92.

34. He, L., et al., Analysis of the brain mural cell transcriptome. Sci Rep, 2016. **6**: p. 35108.

35. Hall, C.N., et al., Capillary pericytes regulate cerebral blood flow in health and disease. Nature, 2014. **508**(7494): p. 55-60.

36. Sweeney, M.D., et al., Blood-Brain Barrier: From Physiology to Disease and Back. Physiol Rev, 2019. **99**(1): p. 21-78.

37. Prinz, M. and J. Priller, The role of peripheral immune cells in the CNS in steady state and disease. Nat Neurosci, 2017. **20**(2): p. 136-144.

38. Engström, L., et al., Lipopolysaccharide-induced fever depends on prostaglandin E2 production specifically in brain endothelial cells. Endocrinology, 2012. **153**(10): p. 4849-61.

39. Miyazaki, K., et al., Disruption of neurovascular unit prior to motor neuron degeneration in amyotrophic lateral sclerosis. Journal of Neuroscience Research, 2011. **89**(5): p. 718-728.

40. Winkler, E.A., et al., Blood-spinal cord barrier breakdown and pericyte reductions in amyotrophic lateral sclerosis. Acta Neuropathol, 2013. **125**(1): p. 111-20.

41. Garbuzova-Davis, S., et al., Impaired blood-brain/spinal cord barrier in ALS patients. Brain Res, 2012. **1469**: p. 114-28.

42. Barten, D.M. and N.H. Ruddle, Vascular cell adhesion molecule-1 modulation by tumor necrosis factor in experimental allergic encephalomyelitis. Journal of Neuroimmunology, 1994. **51**(2): p. 123-133.

43. Wong, D., R. Prameya, and K. Dorovini-Zis, In Vitro Adhesion and Migration of T Lymphocytes Across Monolayers of Human Brain Microvessel Endothelial Cells: Regulation by ICAM-1, VCAM-1, E-selectin and PECAM-1. Journal of Neuropathology & Experimental Neurology, 1999. **58**(2): p. 138-152.

44. Raine, C.S., et al., Homing to central nervous system vasculature by antigen-specific lymphocytes. II. Lymphocyte/endothelial cell adhesion during the initial stages of autoimmune demyelination. Laboratory investigation; a journal of technical methods and pathology, 1990. **63**(4): p. 476-489.

45. Tighe, D., R. Moss, and D. Bennett, Cell surface adrenergic receptor stimulation modifies the endothelial response to SIRS. Systemic Inflammatory Response Syndrome. New Horiz, 1996. **4**(4): p. 426-42.

46. Carlyle Clawson, C., J. Francis Hartmann, and R.L. Vernier, Electron microscopy of the effect of gram-negative endotoxin on the blood-brain barrier. Journal of Comparative Neurology, 1966. **127**(2): p. 183-197.

47. Pluta, R., Pathological opening of the blood-brain barrier to horseradish peroxidase and amyloid precursor protein following ischemia-reperfusion brain injury. Chemotherapy, 2005. **51**(4): p. 223-6.

48. Pluta, R., et al., Early blood-brain barrier changes in the rat following transient complete cerebral ischemia induced by cardiac arrest. Brain Research, 1994. **633**(1): p. 41-52.

49. Kim, K.S., C.A. Wass, and A.S. Cross, Blood–Brain Barrier Permeability during the Development of Experimental Bacterial Meningitis in the Rat. Experimental Neurology, 1997. **145**(1): p. 253-257.

50. Arshi, A., et al., Predictors and Sequelae of Postoperative Delirium in Geriatric Hip Fracture Patients. Geriatric Orthopaedic Surgery & Rehabilitation, 2018. **9**: p. 2151459318814823.

51. Maillard, L.C., Action des acides amines sur les sucres : formation des melanoidines par voie methodique. C R Acad Sci, 1912. **154**: p. 66-68.

52. Bennmann, D., et al., Advanced Glycation Endproducts Interfere with Adhesion and Neurite Outgrowth. PLOS ONE, 2014. **9**(11): p. e112115.

53. Gkogkolou, P. and M. Böhm, Advanced glycation end products. Dermato-Endocrinology, 2012. **4**(3): p. 259-270.

54. Miklós Péter Kalapos, METHYLGLYOXAL AND GLUCOSE METABOLISM: A HISTORICAL PERSPECTIVE AND FUTURE AVENUES FOR RESEARCH. Drug Metabolism and Drug Interactions, 2008. **23**(1-2): p. 69-92.

55. Ahmed, N., et al., Increased formation of methylglyoxal and protein glycation, oxidation and nitrosation in triosephosphate isomerase deficiency. Biochimica et Biophysica Acta (BBA) - Molecular Basis of Disease, 2003. **1639**(2): p. 121-132.

56. Ramasamy, R., et al., Advanced glycation end products and RAGE: a common thread in aging, diabetes, neurodegeneration, and inflammation. Glycobiology, 2005. **15**(7): p. 16R-28R.

57. Meredith, M.E., Z.-C. Qu, and J.M. May, Ascorbate reverses high glucose- and RAGE-induced leak of the endothelial permeability barrier. Biochemical and Biophysical Research Communications, 2014. **445**(1): p. 30-35.

58. Schraag, S., et al., Propofol vs. inhalational agents to maintain general anaesthesia in ambulatory and in-patient surgery: a systematic review and meta-analysis. BMC Anesthesiol, 2018. **18**(1): p. 162.

59. Asserhøj, L.L., et al., No evidence for contraindications to the use of propofol in adults allergic to egg, soy or peanut†. Br J Anaesth, 2016. **116**(1): p. 77-82.

60. Baker, M.T. and M. Naguib, Propofol: the challenges of formulation. Anesthesiology, 2005. **103**(4): p. 860-76.

61. Tang, P. and R. Eckenhoff, Recent progress on the molecular pharmacology of propofol. F1000Res, 2018. **7**: p. 123.

62. Fiset, P., et al., Brain mechanisms of propofol-induced loss of consciousness in humans: a positron emission tomographic study. J Neurosci, 1999. **19**(13): p. 5506-13.

63. Leung, L.S., et al., Brain areas that influence general anesthesia. Prog Neurobiol, 2014. **122**: p. 24-44.

64. Sahinovic, M.M., M. Struys, and A.R. Absalom, Clinical Pharmacokinetics and Pharmacodynamics of Propofol. Clin Pharmacokinet, 2018. **57**(12): p. 1539-1558.

65. Li, Y., et al., Propofol Prevents Renal Ischemia-Reperfusion Injury via Inhibiting the Oxidative Stress Pathways. Cellular Physiology and Biochemistry, 2015. **37**(1): p. 14-26.

66. Jovic, M., et al., Mitochondrial molecular basis of sevoflurane and propofol cardioprotection in patients undergoing aortic valve replacement with cardiopulmonary bypass. Cell Physiol Biochem, 2012. **29**(1-2): p. 131-42.

67. Corcoran, T.B., et al., The effects of propofol on neutrophil function, lipid peroxidation and inflammatory response during elective coronary artery bypass grafting in patients with impaired ventricular function. British Journal of Anaesthesia, 2006. **97**(6): p. 825-831.

68. Fischer, S., et al., [In vitro effects of anaesthetic agents on the blood-brain barrier]. Anaesthesist, 2004. **53**(12): p. 1177-84.

69. Zhou, D., et al., Propofol Alleviates DNA Damage Induced by Oxygen Glucose Deprivation and Reperfusion via FoxO1 Nuclear Translocation in H9c2 Cells. Front Physiol, 2019. **10**: p. 223.

70. Huang, Z., et al., The Protective Effects of Benzbromarone Against Propofol-Induced Inflammation and Injury in Human Brain Microvascular Endothelial Cells (HBMVECs). Neurotox Res, 2021. **39**(5): p. 1449-1458.

71. Pape, H.-C., A. Kurtz, and S. Silbernagl, Physiologie. 2014.

72. Lüllmann, H., et al., Pharmakologie und Toxikologie. 2016.

73. Harik, S.I. and T. McGunigal Jr, The protective influence of the locus ceruleus on the blood-brain barrier. Annals of Neurology, 1984. **15**(6): p. 568-574.

74. Ittner, C., et al., Increased Catecholamine Levels and Inflammatory Mediators Alter Barrier Properties of Brain Microvascular Endothelial Cells in vitro. Frontiers in Cardiovascular Medicine, 2020. **7**.

75. Smulter, N., et al., Delirium after cardiac surgery: incidence and risk factors†. Interactive CardioVascular and Thoracic Surgery, 2013. **17**(5): p. 790-796.

76. Kratz, T., et al., The Preventing of Postoperative Delirium. Dtsch Arztebl International, 2015. **112**(17): p. 289-296.

77. Gallinat, J., et al., [Postoperative delirium: risk factors, prophylaxis and treatment]. Anaesthesist, 1999. **48**(8): p. 507-18.

78. Maldonado, J.R., Delirium pathophysiology: An updated hypothesis of the etiology of acute brain failure. International Journal of Geriatric Psychiatry, 2018. **33**(11): p. 1428-1457.

79. Roizen, Michael F., Richard W. Horrigan, and Bryan M. Frazer, Anesthetic Doses Blocking Adrenergic (Stress) and Cardiovascular Responses to Incision—MAC BAR. Anesthesiology, 1981. **54**(5): p. 390-398.

80. Marana, E., et al., Neuroendocrine stress response in gynecological laparoscopy: TIVA with propofol versus sevoflurane anesthesia. Journal of Clinical Anesthesia, 2010. **22**(4): p. 250-255.

81. Deiner, S., et al., Do Stress Markers and Anesthetic Technique Predict Delirium in the Elderly? Dementia and Geriatric Cognitive Disorders, 2014. **38**(5-6): p. 366-374.

82. Acharya, N.K., et al., Sevoflurane and Isoflurane induce structural changes in brain vascular endothelial cells and increase blood−brain barrier permeability: Possible link to postoperative delirium and cognitive decline. Brain Research, 2015. **1620**: p. 29-41.

83. Yasuda, Y., et al., Relationship Between Serum Norepinephrine Levels at ICU Admission and the Risk of ICU-Acquired Delirium: Secondary Analysis of the Melatonin Evaluation of Lowered Inflammation of ICU Trial. Critical Care Explorations, 2020. **2**(2): p. e0082.

84. Yang, S., et al., Anesthesia and Surgery Impair Blood–Brain Barrier and Cognitive Function in Mice. Frontiers in Immunology, 2017. **8**.

85. Lu, S.-M., et al., S100A8 contributes to postoperative cognitive dysfunction in mice undergoing tibial fracture surgery by activating the TLR4/MyD88 pathway. Brain, Behavior, and Immunity, 2015. **44**: p. 221-234.

86. Terrando, N., et al., Systemic HMGB1 Neutralization Prevents Postoperative Neurocognitive Dysfunction in Aged Rats. Frontiers in Immunology, 2016. **7**.

87. Olotu, C., Postoperative neurocognitive disorders. Current Opinion in Anesthesiology, 2020. **33**(1).

88. Alam, A., et al., Surgery, neuroinflammation and cognitive impairment. EBioMedicine, 2018. **37**: p. 547-556.

89. Li, Y., et al., Deferoxamine regulates neuroinflammation and iron homeostasis in a mouse model of postoperative cognitive dysfunction. Journal of Neuroinflammation, 2016. **13**(1): p. 268.

90. Bonaz, B., V. Sinniger, and S. Pellissier, Anti-inflammatory properties of the vagus nerve: potential therapeutic implications of vagus nerve stimulation. The Journal of Physiology, 2016. **594**(20): p. 5781-5790.

91. Rossi, A., et al., Serum Anticholinergic Activity and Postoperative Cognitive Dysfunction in Elderly Patients. Anesthesia & Analgesia, 2014. **119**(4): p. 947-955.

92. Hshieh, T.T., et al., Cholinergic Deficiency Hypothesis in Delirium: A Synthesis of Current Evidence. The Journals of Gerontology: Series A, 2008. **63**(7): p. 764-772.

93. Dickstein, D.L., et al., Changes in the structural complexity of the aged brain. Aging Cell, 2007. **6**(3): p. 275-284.

94. Hussain, M., et al., Novel insights in the dysfunction of human blood-brain barrier after glycation. Mechanisms of Ageing and Development, 2016. **155**: p. 48-54.

95. Li, Q., et al., Advanced glycation end products induce moesin phosphorylation in murine brain endothelium. Brain Research, 2011. **1373**: p. 1-10.

96. Shimizu, F., et al., Advanced glycation end-products disrupt the blood–brain barrier by stimulating the release of transforming growth factor–β by pericytes and vascular endothelial growth factor and matrix metalloproteinase–2 by endothelial cells in vitro. Neurobiology of Aging, 2013. **34**(7): p. 1902-1912.

97. Schut, E.S., et al., Hyperglycemia in bacterial meningitis: a prospective cohort study. BMC Infect Dis, 2009. **9**: p. 57.

98. van Veen, K.E.B., et al., Bacterial meningitis in diabetes patients: a population-based prospective study. Scientific Reports, 2016. **6**(1): p. 36996.

99. Sharma, S.H., et al., Propofol Promotes Blood-Brain Barrier Breakdown and Heat Shock Protein (HSP 72 kd) Activation in the Developing Mouse Brain. CNS & Neurological Disorders - Drug Targets, 2014. **13**(9): p. 1595-1603.

100. Doronzio, A., et al., Postoperative delirium after anestesia with propofol, sevoflurane or desflurane: The Pinocchio trial. Interim analysis of safety and preliminary results: 7AP3-6. European Journal of Anaesthesiology | EJA, 2013. **30**.

101. Yasuda, Y., et al., Relationship Between Serum Norepinephrine Levels at ICU Admission and the Risk of ICU-Acquired Delirium: Secondary Analysis of the

Melatonin Evaluation of Lowered Inflammation of ICU Trial. Critical Care Explorations, 2020. **2**(2).

102. Windmann, V., et al., Intraoperative hyperglycemia increases the incidence of postoperative delirium. Minerva Anestesiol, 2019. **85**(11): p. 1201-1210.
103. Krone, C.A. and J.T.A. Ely, Ascorbic acid, glycation, glycohemoglobin and aging. Medical Hypotheses, 2004. **62**(2): p. 275-279.
104. Hill, A., et al., Vitamin C to Improve Organ Dysfunction in Cardiac Surgery Patients—Review and Pragmatic Approach. Nutrients, 2018. **10**(8): p. 974.
105. Roy, J., et al., Physiological role of reactive oxygen species as promoters of natural defenses. The FASEB Journal, 2017. **31**(9): p. 3729-3745.
106. Volpe, C.M.O., et al., Cellular death, reactive oxygen species (ROS) and diabetic complications. Cell Death & Disease, 2018. **9**(2): p. 119.
107. Vinson, J.A. and T.B. Howard, Inhibition of protein glycation and advanced glycation end products by ascorbic acid and other vitamins and nutrients. The Journal of Nutritional Biochemistry, 1996. **7**(12): p. 659-663.
108. Hughes, J.M., et al., The Effects of Propofol on a Human in vitro Blood-Brain Barrier Model. Frontiers in Cellular Neuroscience, 2022. **16**.
109. van Vliet, E.A., et al., Long-lasting blood-brain barrier dysfunction and neuroinflammation after traumatic brain injury. Neurobiology of Disease, 2020. **145**: p. 105080.
110. Sharma, A., K. Singh, and A. Almasan, Histone H2AX phosphorylation: a marker for DNA damage. Methods Mol Biol, 2012. **920**: p. 613-26.
111. Tarrade, S., et al., Histone H2AX Is Involved in FoxO3a-Mediated Transcriptional Responses to Ionizing Radiation to Maintain Genome Stability. International Journal of Molecular Sciences, 2015. **16**(12): p. 29996-30014.
112. Kim, J.L., N.E. Bulthuis, and H.A. Cameron, The Effects of Anesthesia on Adult Hippocampal Neurogenesis. Frontiers in Neuroscience, 2020. **14**.
113. Han, D., et al., Long-term action of propofol on cognitive function and hippocampal neuroapoptosis in neonatal rats. Int J Clin Exp Med, 2015. **8**(7): p. 10696-704.
114. Harrison, P.M. and P. Arosio, The ferritins: molecular properties, iron storage function and cellular regulation. Biochimica et Biophysica Acta (BBA) - Bioenergetics, 1996. **1275**(3): p. 161-203.
115. Killilea, D.W., et al., Iron Accumulation during Cellular Senescence. Annals of the New York Academy of Sciences, 2004. **1019**(1): p. 365-367.
116. Friedman, A., et al., Ferritin as an important player in neurodegeneration. Parkinsonism & Related Disorders, 2011. **17**(6): p. 423-430.
117. Molina-Jijón, E., et al., Oxidative stress induces claudin-2 nitration in experimental type 1 diabetic nephropathy. Free Radical Biology and Medicine, 2014. **72**: p. 162-175.
118. Shiomi, R., et al., CaMKII regulates the strength of the epithelial barrier. Scientific Reports, 2015. **5**(1): p. 13262.

119. Marunaka, K., et al., The RING finger- and PDZ domain-containing protein PDZRN3 controls localization of the Mg²⁺ regulator claudin-16 in renal tube epithelial cells. Journal of Biological Chemistry, 2017. **292**(31): p. 13034-13044.

120. Heiler, S., et al., The importance of claudin-7 palmitoylation on membrane subdomain localization and metastasis-promoting activities. Cell Communication and Signaling, 2015. **13**(1): p. 29.

121. Reiche, J. and O. Huber, Post-translational modifications of tight junction transmembrane proteins and their direct effect on barrier function. Biochimica et Biophysica Acta (BBA) - Biomembranes, 2020. **1862**(9): p. 183330.

122. Olsen, J.V., et al., Quantitative Phosphoproteomics Reveals Widespread Full Phosphorylation Site Occupancy During Mitosis. Science Signaling, 2010. **3**(104): p. ra3-ra3.

123. Han, G., et al., Large-scale phosphoproteome analysis of human liver tissue by enrichment and fractionation of phosphopeptides with strong anion exchange chromatography. PROTEOMICS, 2008. **8**(7): p. 1346-1361.

4. Thesen

1. Glykierung des Endothels führt zu erhöhter Permeabilität.
2. Advanced Glycation Endproducts (AGE) verstärken Effekte von Noradrenalin und Propofol auf die Permeabilität.
3. Ascorbinsäure hat protektive Effekte auf die Permeabilitätserhöhung durch AGE.
4. Die Permeabilität für kleine Moleküle steigt durch Propofol-Einfluss.
5. Propofol beeinflusst über das Protein H2AX die Erkennung von DNA-Schäden.
6. Propofol beeinflusst den Eisenstoffwechsel über eine Erhöhung von Ferritin.
7. Propofol hat keine Auswirkungen auf die Expression von Zell-Zell-Kontakten.
8. Propofol führt zu Veränderungen auf Proteomebene, die eine Rolle bei der Entstehung des postoperativen Delirs spielen können.

Publikationsteil

1. Weber V, Olzscha H, Längrich T, Hartmann C, Jung M, Hofmann B, Horstkorte R, Bork K. Glycation Increases the Risk of Microbial Traversal through an Endothelial Model of the Human Blood-Brain Barrier after Use of Anesthetics. *Journal of Clinical Medicine*. 2020; 9(11):3672. https://doi.org/10.3390/jcm9113672

2. Längrich T, Bork K, Horstkorte R, Weber V, Hofmann B, Fuszard M, Olzscha H. Disturbance of Key Cellular Subproteomes upon Propofol Treatment Is Associated with Increased Permeability of the Blood-Brain Barrier. *Proteomes*. 2022; 10(3):28. https://doi.org/10.3390/proteomes10030028

Journal of
Clinical Medicine

MDPI

Article

Glycation Increases the Risk of Microbial Traversal through an Endothelial Model of the Human Blood-Brain Barrier after Use of Anesthetics

Veronika Weber [1,†], Heidi Olzscha [1,*,†], Timo Längrich [1], Carla Hartmann [2], Matthias Jung [2], Britt Hofmann [3], Rüdiger Horstkorte [1] and Kaya Bork [1]

1 Institut für Physiologische Chemie, Martin-Luther-Universität Halle-Wittenberg, Hollystr. 1, 06114 Halle (Saale), Germany; veronika.weber@uk-halle.de (V.W.); timo.laengrich@uk-halle.de (T.L.); ruediger.horstkorte@uk-halle.de (R.H.); kaya.bork@uk-halle.de (K.B.)
2 Klinik und Poliklinik für Psychiatrie, Psychotherapie und Psychosomatik, Martin-Luther-Universität Halle-Wittenberg, Julius-Kühn-Str. 7, 06112 Halle (Saale), Germany; carla.hartmann@uk-halle.de (C.H.); matthias.jung@uk-halle.de (M.J.)
3 Klinik und Poliklinik für Herzchirurgie, Universitätsklinikum Halle (Saale), Ernst-Grube-Str. 20, 06120 Halle (Saale), Germany; britt.hofmann@uk-halle.de
* Correspondence: Heidi.Olzscha@medizin.uni-halle.de; Tel.: +49-345-557-3847
† These authors contributed equally.

Received: 8 October 2020; Accepted: 11 November 2020; Published: 16 November 2020

Abstract: The function of the human blood–brain barrier (BBB), consisting mainly of the basement membrane and microvascular endothelial cells, is to protect the brain and regulate its metabolism. Dysfunction of the BBB can lead to increased permeability, which can be linked with several pathologies, including meningitis, sepsis, and postoperative delirium. Advanced glycation end products (AGE) are non-enzymatic, posttranslational modifications of proteins, which can affect their function. Increased AGE levels are strongly associated with ageing and degenerative diseases including diabetes. Several studies demonstrated that the formation of AGE interfere with the function of the BBB and may change its permeability for soluble compounds. However, it is still unclear whether AGE can facilitate microbial traversal through the BBB and how small compounds including anesthetics modulate this process. Therefore, we developed a cellular model, which allows for the convenient testing of different factors and compounds with a direct correlation to bacterial traversal through the BBB. Our results demonstrate that both glycation and anesthetics interfere with the function of the BBB and promote microbial traversal. Importantly, we also show that the essential nutrient and antioxidant ascorbic acid, commonly known as vitamin C, can reduce the microbial traversal through the BBB and partly reverse the effects of AGE.

Keywords: advanced glycation endproducts (AGE); anesthetics; ascorbic acid; blood–brain barrier; diabetes mellitus; glycation; human brain microvascular endothelial cells; meningitis; microbial traversal; propofol

1. Introduction

Due to the increased life span, age-related diseases, and consecutive demographic changes, health and mental performance in the elderly is becoming more important. The involvement of advanced glycation end products (AGE) is one possible cause for molecular ageing and correlates with the development of age-related diseases, in particular diabetes [1]. During normal ageing, AGE accumulate in the organism, thus contributing to the molecular mechanisms of cellular ageing [2,3]. AGE are built during glycation, a non-enzymatically condensation reaction between the carbonyl group of reducing

carbohydrates or metabolites and free amino groups. The reaction includes the reversible formation of Schiff bases, which further rearrange to so-called Amadori products, and which are finally converted to AGE [4]. Histopathologic studies already showed accumulations of a diversity of AGE in the lung, liver, kidney, or amyloid plaques in Alzheimer's disease [5]. Fragmentation of Amadori products can result in the formation of methylglyoxal (MGO), which is also formed as a regular by-product of glycolysis. Up to 0.4% of all glucose molecules are metabolized to MGO per cycle of glycolysis, whereby concentrations can be even higher in impaired glucose utilization or hyperglycemia [6,7]. MGO is a highly reactive dicarbonyl molecule, leading to the formation of different AGE. In general, the accumulation of dicarbonyl components is also referred to as carbonyl stress [2,8].

The pathology of AGE is mediated through different mechanisms. The generation of protein modifications or cross-links of extra- or intracellular components can alter protein function or even results in a complete loss of protein function [1]. Another aspect to be mentioned is the binding of AGE to receptors, such as the receptor for advanced glycation end products (RAGE), thereby activating pro-inflammatory signal transduction cascades [8]. Endothelial cells cultivated in high glucose concentrations show an increased RAGE activity which leads to increased endothelial cell permeability [9].

Since AGE can basically affect all proteins, they also interfere with proteins of the blood-brain barrier (BBB). The BBB is a tight barrier which separates the blood from the brain, regulates the access of large and hydrophilic molecules to the brain and ensures that the brain can act in a metabolically strictly controlled compartment [10]. The most important cell type forming the tight BBB are the brain microvascular endothelial cells (BMECs). They have some unique features which distinguish them from other endothelial cells, such as a high number of tight junctions and adherens junctions [11] and a continuous basement membrane [12]. There are certain marker proteins for the tight junctions between the BMECs, e.g., occludin, whose level are high in intact BMECs [13]. Another marker protein in BMECs is VE-cadherin, a transmembrane protein which mainly constitutes the adherens junctions and is linked to the actin cytoskeleton with catenins [14]. Many diseases are associated with increased permeability of the BBB, including bacterial meningitis and sepsis [15]. Additionally, iatrogenic disorders can be accompanied with a more permeable BBB, an example would be the postoperative delirium, which is strongly associated with preoperative infections [16,17] and diabetes has been found as independent predisposing factor [18].

Multiple studies have shown that patients with diabetes have a two-fold higher risk of developing meningitis or encephalitis with hyperglycemia remaining a risk factor for severe outcomes and increase of mortality [19–21]. In addition to the immunosuppressing effects of diabetes, there are indications that AGE can be causative for an increased permeability of the BBB and some mechanistic aspects give further evidence for this hypothesis. For instance, Shimizu et al. showed in a study that AGE reduced the expression of claudin 5 in BMECs by increasing autocrine signaling via the vascular endothelial growth factor (VEGF) cascade. They also proposed that AGE increase the degree of autocrine TGF-β signaling by pericytes, and thereby weaken the BBB through the up-regulation of VEGF and MMP-2 in BMECs under diabetic conditions [22]. The expression of the proteins zonula occludens-1 (ZO-1) and occludin is downregulated by MGO in a model built with THBMEC [23]. Another study revealed that AGE can cause phosphorylation of myosin in murine brain microvascular endothelial cells with p38 and Rho kinase pathway activation [24]. Kim et al. showed that the primary entry site of circulating bacteria is the microvessels [25]. However, the BBB prevents the entry of bacteria. The ability of bacteria entering the brain via transcellular as well as paracellular traversal is related to the interaction with proteins which are also affected by AGE, such as VEGF [26,27], ZO-1, or occludin [28].

However, it has not been clarified, so far, how and to what degree AGE can cause an increased permeability of the BBB that even bacteria could traverse easier through the barrier, leading to the mentioned disease of bacterial meningitis. It has also not been systematically evaluated, how compounds affecting the brain, especially anesthetics, can influence the permeability of the BBB. There are studies showing that propofol as a common anesthetic induce cellular stress and support the breakdown of BBB [29,30]. In addition, some studies proof the neuroprotective effect of propofol by tighten the BBB and lower incidence of post-operative delirium compared with other anesthetics such as sevoflurane [31,32].

In this study, we report the usage of a newly developed BBB model system [33] to analyze the effects of AGE on the permeability of the BBB, how this can modulate a propofol response and how bacterial traversal would be affected. We could demonstrate that bacterial traversal increases upon treatment of the cells with physiological doses of an AGE building compound. We also could show that anesthetics such as propofol and supplements in anesthesia including norepinephrine lead to an increase of the BBB permeability for bacteria. Importantly, the antioxidant ascorbic acid, more commonly known as vitamin C, can partly reverse the effects of the AGE building compound, propofol and norepinephrine. Similarly, it has been shown that ascorbic acid has positive effects on the permeability of glycated blood-brain barrier cells measured by transendothelial inulin transfer [9]. We propose that ascorbic acid can be beneficial in reducing the effects of diabetic encephalopathy which is accepted as an important complication of diabetes and preventing adverse effects on the BBB during anesthesia.

The BBB is a tight barrier separating brain parenchyma from circulating blood, whereas building of AGE lead to an increase of microbial traversal through human brain microvascular endothelial cells.

2. Experimental Section

2.1. Cells and Cell Culture

Transfected human brain microvascular endothelial cells (THBMEC) [34] were kindly provided by the group of MF Stins (Los Angeles, CA, USA). Cells were cultivated in DMEM F12 medium (Thermo Fisher Scientific, Waltham, MA, USA) at 37 °C in a humidified cell culture incubator. Supplemented medium was prepared by adding 100 mg/L penicillin and 100 mg/L streptomycin (Thermo Fisher Scientific), 2 mM L-glutamine (Thermo Fisher Scientific) and 4% heat-inactivated fetal calf serum (GE Healthcare, Little Chalfont, UK). Cells were passaged every 3–4 days. THBMECs were detached with Trypsin/EDTA (Thermo Fisher Scientific) and pelleted at 210 g for 3 min. Further particulars can be found in [33].

2.2. Treatment for Immunoblotting

For the immunoblots showing glycation of cells, THMBECs were incubated in medium supplemented with methylglyoxal (MGO) (Sigma Aldrich, St. Louis, MO, USA) for 1 h. Different concentrations, i.e., 0.05 mM, 0.15 mM, 0.45 mM, or 1 mM, of MGO were used for immunoblotting. Additionally, an immunoblot for detection of CD31 was performed. Therefore, cells were incubated with medium supplemented with interleukin 1β (IL1β) (Immunotools, Friesoythe, GER) and tumor necrosis factor α (TNFα) (Immunotools) for 24 h. A concentration of 0.05 ng/mL was used. Cells were incubated in a humidified incubator at 37 °C. Untreated THBMECs cultured in media served as a control.

2.3. Preparation of Cell Extracts

After incubation, treated and control cells were washed twice with PBS. Cells were removed from the surface by scraping and directly lysed into SDS-sample buffer (100 mL buffer containing 12.5% SDS, 0.3 M Tris, 50 mL glycerin, bromophenol blue at pH 6.8 and 1:10 DTT to buffer) which was pre-warmed for 5 min by 90 °C. After mixing, the cell extracts were used for downstream analysis.

2.4. Immunoblotting

Proteins of the samples were separated by SDS-PAGE on a 10% acrylamide gel and transferred afterwards to a nitrocellulose membrane for 1 h 15 min in blotting buffer with a constant amperage of 25 mA per gel. During the blotting process, the blot chamber (VWR, Radnor, PA, USA) was cooled down to avoid overheating. The following staining with ponceau red solution containing 0.1% ponceau S (Carl Roth, Karlsruhe, Germany), 3% trichloroacetic acid and 3% sulfosalicylic acid proved a successful protein transfer on to the membrane. The membrane was washed twice with water and was then blocked for 1 h at room temperature using 5% milk in TBS. The membrane was then incubated with the primary antibodies overnight at 4 °C. Glycation was detected by the monoclonal antibody

CML-26 (ab12514, Abcam, Cambridge, CB2 0AX, UK) at a 1:10,000 dilution. CD31 was detected using the monoclonal anti-CD31-Antibody (ab24590, Abcam) at a dilution of 1:1000. VE-cadherin was detected by a monoclonal antibody (ab166715, Abcam), diluted 1:1000. Occludin was detected using anti-occludin-Antibody (ab167161, Abcam) at a 1:100,000 dilution. To detect integrin-β1, the membrane was blocked for 1 h at room temperature using 5% bovine serum albumin (BSA) (Carl Roth) in TBS. Afterwards, the membrane was incubated with anti-integrin-β1-antibody (Cell Signaling Technology, Frankfurt a. M., Germany diluted 1:1000 in BSA. After incubation with primary antibody, the membrane was washed three times with 1 x PBS for 10 min and incubated with the corresponding peroxidase-conjugated secondary antibody. Therefore, a monoclonal mouse-antibody (ab6789, Abcam) diluted 1:10,000 or rabbit-antibody (ab6721, Abcam) diluted 1:20,000 were used. The proteins were detected using Luminata Forte Western HRP-Substrate (Merck Millipore, Billerica, MA, USA) and signals were visualized using the ChemiDoc MP Imaging System (BioRad, Hercules, CA, USA). Occurring bands were analyzed using the associated ImageLab software (BioRad). Ponceau S staining served as loading control and was used to normalize the band intensity of the Western blot. The total protein normalization was recommended by the software producer as a better alternative to housekeeping protein normalization.

2.5. MTT-Assay

MTT assays were performed to determine the cytotoxicity of different cell treatments by measuring the metabolic activity. THBMECs were seeded into 96-well microtiter plates at a density of 1×10^5 per well and treated with 0.15 mM MGO for 1 h, 3 µg/mL propofol (propofol 2%, Fresenius Kabi, SGP) for 3 h or 1 ng/mL norepinephrine (Arterenol® 1 mg/mL, Sanofi-Aventis, Frankfurt a.M., GER) for 1 h added to medium. After treatment cells were washed with 200 µL PBS per well. MTT (Sigma, Saint Louis, MO, USA) was diluted to a concentration of 0.5 mg/mL in normal medium and 100 µL were added to each well and incubated for 4 h in a humidified incubator. After removal of MTT containing medium, remaining formazan crystals were dissolved in 150 µL DMSO (Sigma, Saint Louis, MO, USA). The absorbance was measured photometrically at a wavelength of 570 nm (background 630 nm) on a microplate reader Multiskan EX (Thermo Fisher Scientific, Rockford, IL, USA). Relative cell viability was calculated and compared to the untreated control, which were set to 100% of metabolic activity.

2.6. Measurement of Bacterial Traversal through the BBB

To test the effect of different compounds on the permeability of the human BBB, we developed an endothelial cell culture model, which mimics a tight BBB model with THBMECs. Cells were treated and exposed to bacteria as previously described [33]. In brief, THBMECs were grown on 12-well filters with 3.0-µm pore size (ThinCerts, Greiner Bio-One, Austria) to a confluent layer. Before seeding cells, filters were coated with 10 µg/mL collagen IV and 10 µg/mL fibronectin (Sigma, Saint Louis, MO, USA) mixture for 24 h. The cells were incubated for 14 days in a cell culture incubator with 5% CO_2 atmosphere at 37 °C, changing the DMEM/F12 medium every 2 to 3 days in the upper and lower chamber. Afterwards, they were treated with the different compounds. In the next step, medium from both chambers was changed to antibiotic free DMEM/F12 medium and *E. coli* strain GM2163 (Fermentas Life Sciences, Lithuania) bacteria were then fed into the upper chamber. After 6 h, samples from the lower chamber were plated and colonies were counted.

2.7. Treatment for Measurement of Bacterial Traversal through the BBB

To treat the cell monolayer in our model, THBMECs were grown for 14 days to confluence which were proofed by evaluating cell density on the filters with a microscope. Exemplarily, we measured the transendothelial electrical resistance (TEER) of 70 $\Omega \cdot cm^2$ after growing on filters for 14 days (Supplementary Figure S1). Afterwards, THBMECS were incubated in medium supplemented with different compounds. To test the effect of glycation, cells were washed with PBS and medium supplemented with 0.15 mM MGO was given into the upper and lower chamber for 1 h. To test the

effect of anesthetics, cells were washed with PBS and medium where 3 µg/mL propofol for 3 h or 1 ng/mL norepinephrine were given into both chambers for 1 h. Incubation in medium supplemented with Intralipid (SMO Flipid 200 mg/mL, Fresenius Kabi) for 3 h and sodium metabisulfite for 1 h (PanReacAppliChem, ITW Reagents, Darmstadt, GER) served as control. To test the effect of vitamin C, cells were incubated with 0.1 mM ascorbic acid (AA) (Carl Roth) for 4 h added to medium in both chambers. Additionally, cells were first incubated with medium supplemented with 0.15 mM MGO and afterwards they were washed with PBS and medium supplemented with 0.1 mM AA were added. In addition, the reverse procedure was performed with AA treatment first followed by treatment with MGO. Untreated cells served as control.

2.8. RNA Extraction and Barrier Genes High-Throughput Multiplex qPCR

RNA was isolated using the NucleoSpinTM RNA kit according to manufacturer's protocol (Macherey-Nagel, Cat. No. 740955.250) from the indicated cell lines. Samples of 250 ng RNA were transcribed to cDNA using the High-Capacity cDNA Reverse 191 Transcription Kit (Applied Biosystems, Cat. No. 4368814), according to the manufacturer's instructions. Targets were preamplified using tenfold concentrated primer pools, mastermix, and the following program: 15 min at 95 °C for HotStar Plus Taq Polymerase (Qiagen, Cat. No. 203603), 18 cycles of 40 s at 95 °C, 40 s at 60 °C, 80 s at 72 °C, and 7 min at 72 °C. We used a BiomarkTM system containing an IFC Controller HX and 96.96 Dynamic ArraysTM IFC, according to the manufacturer's instructions. In brief, each sample well was loaded with TagmanTM gene expression mastermix, DNA binding dye sample loading reagent, EvaGreenTM binding dye, and 1:8 diluted preamplified cDNA. Target wells were loaded with assay loading reagent and the respective primers. After qPCR and data allocation, the Ct values of the targets were normalized to the endogenous control B2M. The ΔCt values were used for the following statistical analysis applying the software Graph Pad Prism 7 (GraphPad, San Diego, CA, USA).

2.9. Statistical Analysis

Data are represented as bar diagrams or data points including mean ± standard error of measurement (SEM). Statistical analyses were performed using OriginPro2017 software (OriginLab Corporation, Northampton, MA, USA) or Graph Pad Prism 7 (GraphPad, San Diego, CA, USA). Unpaired student t-test against the control group or a theoretical value of 1 (due to data normalization) was used for microbial traversal after treatment with MGO. ANOVA and Tukey Kramer as post hoc tests were used for every other data. A difference between untreated and treated samples at $p < 0.05$ was considered as statistically significant, and significant p-values are displayed on each graph. RNA extraction and barrier genes high-throughput multiplex qPCR has been performed in two technical replicates for each cell line.

3. Results

In order to analyze the effects of glycation and anesthetics on bacterial traversal through the BBB, a model, which mimics the BBB, was built-up by human brain endothelial cells (THBMEC) [33,34]. These cells were grown on filters until confluence to prevent bacteria in the upper chamber from crossing into the lower chamber. Since this barrier is built-up by cell junctions of THBMECs, we firstly characterized the expression of common tight and adherens junction proteins at the beginning and end of the two weeks of cell cultivation.

3.1. Determination of Protein Levels Building the Cell Junctions

Occludin is an important protein of tight junctions, therefore we decided to analyze their levels by immunoblotting. There was a significant increase of occludin expression between day 2 and 16 (Figure 1a). VE-cadherin as a representative protein of adherens junctions increased between day 2 and 16 as well (Figure 1b). Integrin-β1 did not display increased expression over time (Figure 1c), but was also an important protein for cell adherence and cell signaling. We also treated the cells for 24 h with interleukin-1-beta (IL1β) and tumor necrosis factor alpha (TNFα) to analyze, whether THBMECs were

able to react on proinflammatory mediators. A marker for this event was the platelet endothelial cell adherence molecule (PECAM or CD31), which primarily regulates leukocyte transmigration. The expression of CD31 increased regardless of whether using concentrations of 0.05 ng/mL or 10 ng/mL of IL1β or TNFα (Figure 1d), as proven by immunoblotting. The presence of mRNA coding for various other proteins with crucial functions in building tight junctions could be confirmed by qPCR in the THBMECs compared to hCMECs/D3 cells (Supplementary Figure S2).

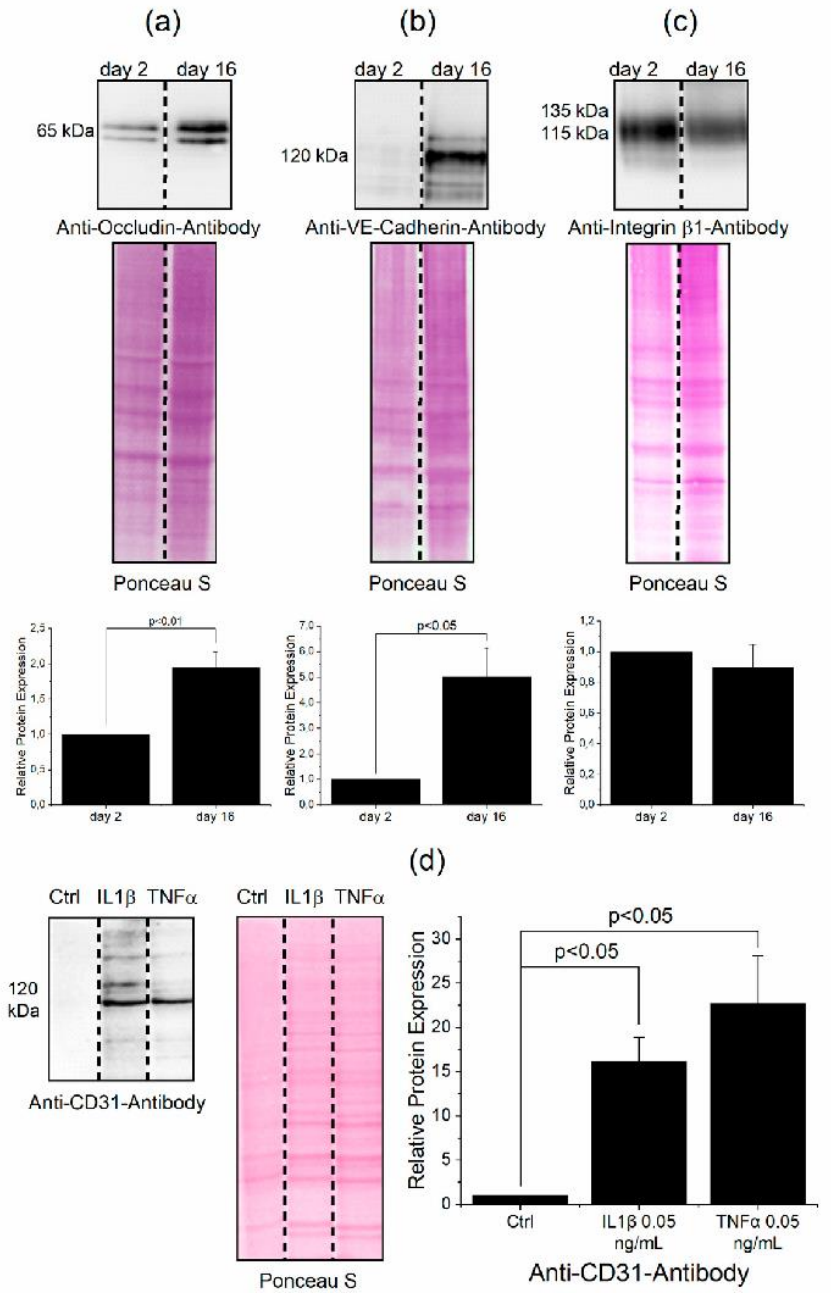

Figure 1. Determination of protein levels building the cell junctions in THMBECs. THBMECs were cultivated for 2 and 16 days. Afterwards, total protein was isolated and separated using SDS-PAGE. Expression of proteins was detected via immuno-blotting using anti-occludin antibody (**a**), anti-VE-cadherin antibody (**b**) and anti-integrin β1 antibody (**c**), respectively ($n = 3$). THBMECs were incubated with IL1β and TNFα at a concentration of 0.05 ng/mL for 24 h. Total protein was isolated and separated using SDS-PAGE. Expression of CD31 was detected by immuno-blotting using anti-CD31 antibody (**d**), ($n = 3$).

3.2. Protein Glycation Is Induced by MGO

To analyze the effect of glycation on cells, we treated them with MGO to induce formation of AGE. The treatment lasted 1 h and different concentrations of MGO were used to find the lowest AGE inducing concentration for further experiments. AGE were detected by immunoblotting after treatment with 0.05 mM, 0.15 mM, 0.45 mM, or 1 mM MGO (Figure 2a). The immunoblots were quantitated (Figure 2b). According to the results, we decided to use 0.15 mM MGO for 1 h in all our further experiments, since these concentrations have been measured in patients [35]. Additionally, cell viability assays were performed to assess the treatment of cells with 0.15 mM MGO for 1 h. The assay did not show toxic effects of 0.15 mM MGO treatment for 1 h on THBMECs or interference with cellular proliferation (Figure 2d). Untreated cells served as control in this assay. We also tested whether the expression levels of RAGE change during the treatment and whether the Western blot signal would be masked by AGE. We could detect RAGE in the THBMECs by immunoblotting with or without treatment of MGO, whereby the protein level did not change after an hour of treatment with MGO (Supplementary Figure S3).

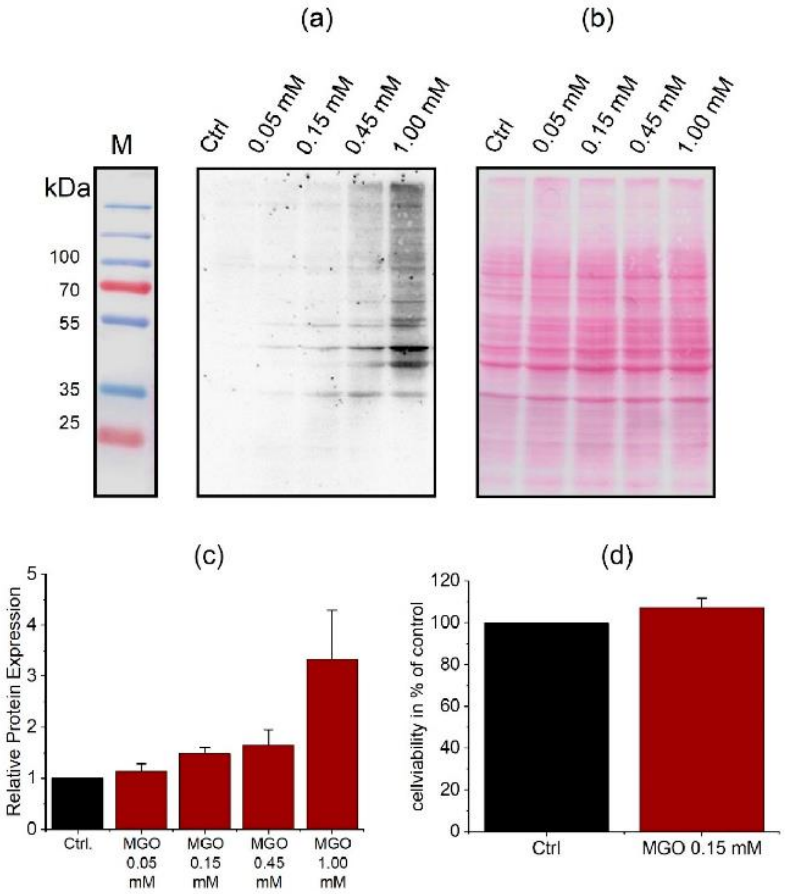

Figure 2. THBMECs were incubated with MGO at different concentrations for 1 h in normal medium. Total protein was isolated and separated using SDS-PAGE. Glycation of proteins was detected by immuno-blotting using anti-AGE-antibody (CML-26) (**a**). Ponceau S staining served as loading control (**b**). The bar graph shows the mean + SEM of relative protein glycation detected by immunoblotting, untreated cells serve as control (**c**), (n = 5). Cell viability in THBMECs upon treatment with MGO (**d**). Cells were treated with 0.15 mM MGO for 1 h. Afterwards, MTT assays were performed. The graph shows the mean + SEM of the absorbance of formazan crystals at a wavelength of 570 nm, untreated cells served as control, (n = 3).

3.3. Protein Glycation Increases the Permeability of the BBB, Which Can Be Reverted by Antioxidant

In order to analyze the effect of glycation on bacterial traversal, we built the model of human BBB with THBMECs and after cultivation of 14 days, cells were treated with 0.15 mM MGO for 1 h. The upper chamber was then inoculated with bacteria and, after 6 h, medium from the lower chamber was plated and colonies were counted. Untreated cells served as control and showed a low bacterial traversal with 6.2 colonies on average. Compared to this 0.15 mM MGO for 1 h affected the traversal by increasing the number of colonies up to 47 colonies on average (Figure 3). In addition, we wanted to test some compounds with anti-glycation effects in our model of the human blood-brain barrier. An agent we took into consideration fulfilling the requirement was ascorbic acid (AA), better known as vitamin C. It is a reducing agent, but in addition, it provided the risk of glycation by itself [36]. We used 0.1 mM ascorbic acid for 4 h and MGO with 0.15 mM for 1 h to treat cells after 14 d of cultivation. Additionally, we combined both treatments—first ascorbic acid then MGO or vice versa. The glycated cells with the additional ascorbic acid treatment showed a significant decrease of microbial traversal compared to cells, which were only treated with MGO (Figure 3).

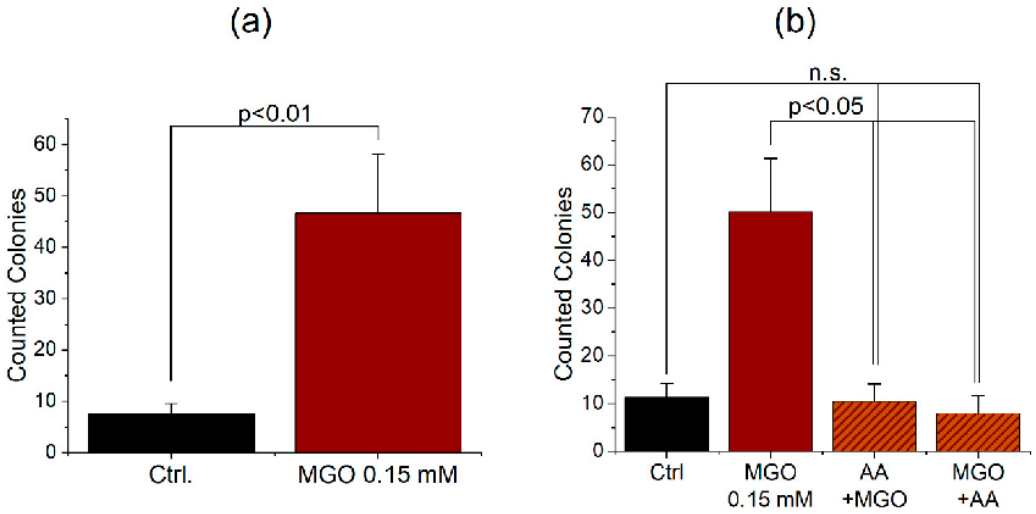

Figure 3. Increased microbial traversal through a BBB model upon treatment with MGO (**a**). THBMECs were treated with 0.15 mM MGO for 1 h. 450 µL of bacteria suspension (OD 0.5) were put into each upper chamber. Medium from the lower chamber was plated on agar plates after 6 h. Graphs show the mean + SEM of counted colonies, untreated cells serve as control, (n = 3). Microbial traversal in the presence of ascorbic acid decreased in MGO-treated cells (**b**). THBMECs were treated with 0.15 mM MGO for 1 h. Afterwards, ascorbic acid with a concentration of 0.1 mM was administered to the treated cells. Additionally, cells were first treated with ascorbic acid for 4 h and afterwards glycated with MGO 0.15 mM for 1 h. 450 µL of *E. coli* suspension (OD 0.5) was put into each upper chamber. Medium from the lower chamber was plated on agar plates after 6 h. Graphs show the mean + SEM of counted colonies, untreated cells served as control, (n = 3).

3.4. Anesthetics Increase the Permeability of the BBB and Bacterial Traversal

Anesthetics are known to have an impact on permeability of the human blood-brain barrier. Therefore, we decided to test common anesthetics in the human BBB model. Additionally, we combined glycation and anesthetic treatment to exemplary replicate the situation of an older or diabetic person during surgery. We used propofol (PP) as one of the most common anesthetic compounds and norepinephrine (NE), which is used to compensate for a decrease of blood pressure caused by propofol. Treatment of cells was performed with 3 µg/mL propofol [37,38] and 1 ng/mL norepinephrine [39]. These concentrations are in the range of common blood levels during surgery. The propofol treatment

lasted 3 h to simulate an average surgery. Norepinephrine is mostly used as bolus injection, so we treated cells for 1 h in our model.

Again, we performed cell viability assays for the treatment of cells with propofol 3 µg/mL for 3 h and norepinephrine 1 ng/mL for 1 h. The assay showed no toxic effect of propofol or norepinephrine treatment on THBMECs or interference with proliferation (Figure 4). Untreated cells served as control in this assay. According to the test results, we treated the THBMECs in our model after 14 d cultivation with 3 µg/mL propofol for 3 h or 1 ng/mL norepinephrine for 1 h. To see effects of AGE formation during surgery, we glycated cells first with 0.15 mM MGO for 1 h and treated them with propofol or norepinephrine. After treatment, the bacteria solution was put into the upper chamber and after 6 h, medium from the lower chamber was plated and colonies were counted. Untreated cells served as control. There was a significant increase of microbial traversal between non-glycated and glycated cells treated with propofol. As control, we used a soya oil solution (Intralipid), since common propofol compounds are mixed with soya oil. Additionally, we were able to show an increase of microbial traversal between non-glycated and glycated cells after norepinephrine treatment. Sodium metabisulfite served as control, because it is used for the preservation of norepinephrine.

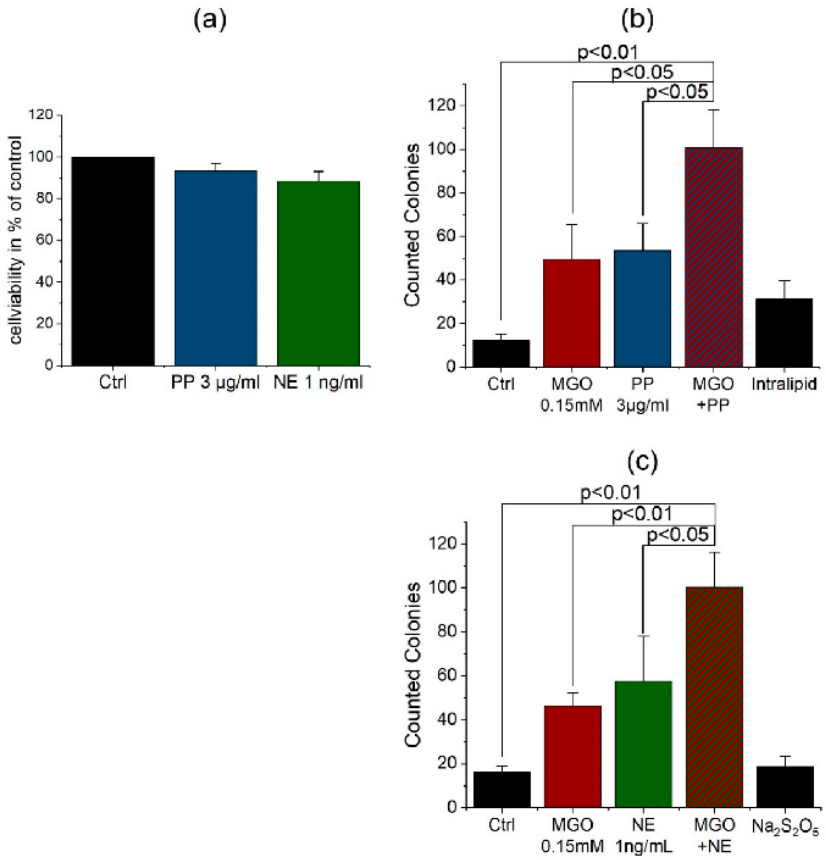

Figure 4. Cell viability of the compounds propofol (PP) and norepinephrine (NE) in endothelial cells (**a**). THBMECs were treated with 3 µg/mL propofol for 3 h and 1 ng/mL norepinephrine for 1 h. MTT assays were performed to analyze the cell viability after treatment. The graph shows the mean + SEM of the cell viability, untreated cells served as control, (n = 3). Microbial traversal in presence of propofol and norepinephrine with and without MGO treatment. THBMECs were treated with 0.15 mM MGO for 1 h. Afterwards, glycated and non-glycated cells were treated with 3 µg/mL propofol for 3 h (**b**) or with 1 ng/mL norepinephrine for 1 h (**c**). 450 µL of *E. coli* suspension (OD 0.5) were put into each upper chamber. Medium from the lower chamber was plated on agar plates after 6 h. The graph shows the mean + SEM of counted colonies, untreated cells and intralipid (**b**) or sodium metabisulfite (**c**) served as control, (n = 3).

4. Discussion

Our results demonstrated the effect of glycation on the permeability of the human blood-brain barrier. As many studies proved a correlation of diabetes with meningitis [19–21] and post-operative delirium (POD) [18], we were able to show an effect of AGE on our model of the human BBB. A significant increase of microbial traversal in the model of the BBB in THBMECs was observed after glycation with MGO. We used a low amount of MGO which did not affect the cell viability as MTT assays (Figure 2d) indicate. This concentration is at the lower range of measured human serum concentrations of MGO (190 +/− 68 nmol/L) [35]. These results indicate an effect of AGE formation on the transcellular and intracellular barrier function of THBMECs, which is associated with paracellular or transcellular traversal of bacteria [22–24]. Furthermore, we measured the transendothelial electrical resistance (TEER) (Supplementary Figure S1) proving that a breakdown of the BBB is not causative for the resulting effects. A decrease of resistance after treatment with MGO, propofol, or norepinephrine could not be measured in our model.

The treatment with propofol and norepinephrine was performed with amounts as similar as possible to plasma concentrations during surgery [37–39]. To show effects in diabetic patients, cells were glycated with MGO before inoculating with bacteria. The single treatment with propofol indicates a damaging effect and a support of the breakdown of BBB as some studies also proposed [29,30]. As the effects of propofol are distinct in our experiments, we cannot confirm neuroprotective effects of propofol as some studies comparing to sevoflurane anesthesia propose [32]. Single treatment with norepinephrine increases the permeability of BBB as well. In animal models, high levels of norepinephrine correlated with POD [40], whereas the circumstances in humans have not been entirely elucidated so far [41]. Whilst norepinephrine is important for maintaining hemodynamical stability in ICU patients, it led to an increase of the microbial traversal across the BBB in THBMECs. The results indicate an additive effect of AGE formation and propofol or norepinephrine on the permeability of human blood-brain barrier (Figure 4). The wide influence of AGE on proteins and the effect of RAGE seem to amplify the negative effect of anesthesia on the permeability of human BBB. As diabetes is associated with a high level of AGE, the results highlight the importance of spare anesthesia in diabetic patients and a well-adjusted blood glucose level before surgery [42].

Since ascorbic acid is a reducing agent [43], it is able to prevent glycation of proteins like hemoglobin [44]. Our results demonstrate that ascorbic acid partly reverses the effect of glycation on the permeability of the human BBB (Figure 3b). Patients after surgery tend to have a high amount of reactive oxygen species (ROS), which often exceed their antioxidant capacity [45]. This leads to damage of macromolecules and ends up in organ dysfunction including POD. Ascorbic acid is known to be one of the most important antioxidants to reduce the influence of free radicals [46] and systemic inflammatory reaction [47]. In addition to the systemic impact of ascorbic acid, our experiments show a positive effect on glycated cells. As hyperglycemia is associated with a high level of ROS [48], ascorbic acid prevents the formation of AGE [49]. Thus, our results indicate an effect of ascorbic acid after the formation of AGE. The human body depends on an adequate intake of vitamin C, as it is unable to synthesize ascorbic acid by itself. Given that 0.1 mM ascorbic acid has been used in the experiments, it reflects a realistic concentration, if 100 mg ascorbic acid are ingested in a person with a blood volume of 4–6 L on average. We propose that high levels of ascorbic acid in the body fluids may have beneficial effects of diabetic encephalopathy, which is accepted to be a major complication of diabetes mellitus and prevent adverse effects during anesthesia.

This model provides the possibility to test the influence of agents on the permeability of the human BBB, whereby the absolute measurement of bacteria traversal across the cell monolayer allows a fast testing to analyze further drugs.

Further research is needed to determine the mainly affected proteins. A screen via mass spectrometry could give first insights of altered protein levels and associated pathways, which could be confirmed with cell biological experiments. The route of the bacteria during the traversal from the

apical side to the basolateral side is also not entirely clear. Thus, tracking experiments and monitoring of the bacteria by microscopy could help to elucidate their routes.

5. Conclusions

In summary, we could demonstrate an increase of microbial traversal across the human BBB after treatment with AGE as well as propofol and norepinephrine in our THBMEC model. Importantly, these results could be partially reversed upon the administration of ascorbic acid, which could have beneficial effects, if given prior to anesthesia.

Supplementary Materials: The following are available online at http://www.mdpi.com/2077-0383/9/11/3672/s1, Figure S1: Measurement of Colony Building Units (CBU) at an optical density with a range from 4.5 to 5.5. at 570 nm (a). Transendothelial electrical resistance measured in the BBB model of THBMEC after different time points and treatments (b, c), Figure S2: Heat map analysis of high-throughput multiplex barrier qPCR data of THBMEC cells in comparison to hCMEC/D3 cells as positive control, set to 1.0. Total RNA extracts were pre-amplified and the Ct values of the targets were normalized to the endogenous control B2M after qPCR, Figure S3: Expression levels of RAGE in THBMECs with or without MGO treatment. THBMECs were incubated with 0.15 mM MGO for 1 h in serum-free medium. Total protein was separated using SDS-PAGE. Expression of RAGE was detected by immuno-blotting using anti-RAGE-antibody (ab3611) (a). Tubulin detected with an anti-tubulin antibody as well as Ponceau S staining served as loading control (b).

Author Contributions: Conceptualization, V.W., H.O., K.B. and R.H.; formal analysis, V.W., H.O., T.L. and C.H.; writing—original draft preparation, H.O. and V.W.; writing—review and editing, V.W., H.O., C.H., K.B., B.H. and R.H.; visualization, V.W.; supervision, M.J., R.H., H.O. and K.B.; project administration, R.H.; funding acquisition, R.H. and B.H. All authors have read and agreed to the published version of the manuscript.

Funding: V.W., H.O. and R.H. were supported by the Deutsche Forschungsgemeinschaft (DFG, Germany) (RTG 2155, ProMoAge). T.L. was supported by the Wilhelm Roux Program HaPKoM.

Acknowledgments: The authors acknowledge Annett Thate for technical assistance.

Conflicts of Interest: The authors declare no conflict of interest.

References

1. Schalkwijk, C.G.; Miyata, T. Early- and advanced non-enzymatic glycation in diabetic vascular complications: The search for therapeutics. *Amino Acids* **2012**, *42*, 1193–1204. [CrossRef] [PubMed]
2. Bennmann, D.; Horstkorte, R.; Hofmann, B.; Jacobs, K.; Navarrete-Santos, A.; Simm, A.; Bork, K.; Gnanapragassam, V.S. Advanced glycation endproducts interfere with adhesion and neurite outgrowth. *PLoS ONE* **2014**, *9*, e112115. [CrossRef] [PubMed]
3. Gkogkolou, P.; Bohm, M. Advanced glycation end products: Key players in skin aging? *Dermatoendocrinology* **2012**, *4*, 259–270. [CrossRef] [PubMed]
4. John, W.G.; Lamb, E.J. The Maillard or browning reaction in diabetes. *Eye* **1993**, *7*, 230–237. [CrossRef] [PubMed]
5. Singh, R.; Barden, A.; Mori, T.; Beilin, L. Advanced glycation end-products: A review. *Diabetologia* **2001**, *44*, 129–146. [CrossRef] [PubMed]
6. Kalapos, M.P. Methylglyoxal and glucose metabolism: A historical perspective and future avenues for research. *Drug Metabol. Drug Interact.* **2008**, *23*, 69–91. [CrossRef]
7. Ahmed, N.; Battah, S.; Karachalias, N.; Babaei-Jadidi, R.; Horanyi, M.; Baroti, K.; Hollan, S.; Thornalley, P.J. Increased formation of methylglyoxal and protein glycation, oxidation and nitrosation in triosephosphate isomerase deficiency. *Biochim. Biophys. Acta* **2003**, *1639*, 121–132. [CrossRef]
8. Vistoli, G.; De Maddis, D.; Cipak, A.; Zarkovic, N.; Carini, M.; Aldini, G. Advanced glycoxidation and lipoxidation end products (AGEs and ALEs): An overview of their mechanisms of formation. *Free Radic. Res.* **2013**, *47*, 3–27. [CrossRef]
9. Meredith, M.E.; Qu, Z.C.; May, J.M. Ascorbate reverses high glucose- and RAGE-induced leak of the endothelial permeability barrier. *Biochem. Biophys. Res. Commun.* **2014**, *445*, 30–35. [CrossRef]
10. Banks, W.A. From blood-brain barrier to blood-brain interface: New opportunities for CNS drug delivery. *Nat. Rev. Drug. Discov.* **2016**, *15*, 275–292. [CrossRef]
11. Brightman, M.W.; Reese, T.S. Junctions between intimately apposed cell membranes in the vertebrate brain. *J. Cell Biol.* **1969**, *40*, 648–677. [CrossRef] [PubMed]

12. Morris, A.W.; Sharp, M.M.; Albargothy, N.J.; Fernandes, R.; Hawkes, C.A.; Verma, A.; Weller, R.O.; Carare, R.O. Vascular basement membranes as pathways for the passage of fluid into and out of the brain. *Acta Neuropathol.* **2016**, *131*, 725–736. [CrossRef] [PubMed]
13. Luissint, A.C.; Artus, C.; Glacial, F.; Ganeshamoorthy, K.; Couraud, P.O. Tight junctions at the blood brain barrier: Physiological architecture and disease-associated dysregulation. *Fluids Barriers CNS* **2012**, *9*, 23. [CrossRef] [PubMed]
14. Harris, E.S.; Nelson, W.J. VE-cadherin: At the front, center, and sides of endothelial cell organization and function. *Curr. Opin. Cell Biol.* **2010**, *22*, 651–658. [CrossRef] [PubMed]
15. Kim, K.S.; Wass, C.A.; Cross, A.S. Blood-brain barrier permeability during the development of experimental bacterial meningitis in the rat. *Exp. Neurol.* **1997**, *145*, 253–257. [CrossRef]
16. Kratz, T.; Heinrich, M.; Schlauß, E.; Diefenbacher, A. Preventing postoperative delirium. *Dtsch. Arztebl. Int.* **2015**, *112*, 289–296. [CrossRef]
17. Margiotta, A.; Bianchetti, A.; Ranieri, P.; Trabucchi, M. Clinical characteristics and risk factors of delirium in demented and not demented elderly medical inpatients. *J. Nutr. Health Aging* **2006**, *10*, 535–539.
18. Smulter, N.; Lingehall, H.C.; Gustafson, Y.; Olofsson, B.; Engstrom, K.G. Delirium after cardiac surgery: Incidence and risk factors. *Interact. Cardiovasc. Thorac. Surg.* **2013**, *17*, 790–796. [CrossRef]
19. van Veen, K.E.; Brouwer, M.C.; van der Ende, A.; van de Beek, D. Bacterial meningitis in diabetes patients: A population-based prospective study. *Sci. Rep.* **2016**, *6*, 36996. [CrossRef]
20. Kalra, S.; Zargar, A.H.; Jain, S.M.; Sethi, B.; Chowdhury, S.; Singh, A.K.; Thomas, N.; Unnikrishnan, A.G.; Thakkar, P.B.; Malve, H. Diabetes insipidus: The other diabetes. *Indian J. Endocrinol. Metab.* **2016**, *20*, 9–21. [CrossRef]
21. Schut, E.S.; Westendorp, W.F.; de Gans, J.; Kruyt, N.D.; Spanjaard, L.; Reitsma, J.B.; van de Beek, D. Hyperglycemia in bacterial meningitis: A prospective cohort study. *BMC Infect. Dis.* **2009**, *9*, 57. [CrossRef] [PubMed]
22. Shimizu, F.; Sano, Y.; Tominaga, O.; Maeda, T.; Abe, M.A.; Kanda, T. Advanced glycation end-products disrupt the blood-brain barrier by stimulating the release of transforming growth factor-beta by pericytes and vascular endothelial growth factor and matrix metalloproteinase-2 by endothelial cells in vitro. *Neurobiol. Aging* **2013**, *34*, 1902–1912. [CrossRef] [PubMed]
23. Hussain, M.; Bork, K.; Gnanapragassam, V.S.; Bennmann, D.; Jacobs, K.; Navarette-Santos, A.; Hofmann, B.; Simm, A.; Danker, K.; Horstkorte, R. Novel insights in the dysfunction of human blood-brain barrier after glycation. *Mech. Ageing Dev.* **2016**, *155*, 48–54. [CrossRef] [PubMed]
24. Li, Q.; Liu, H.; Du, J.; Chen, B.; Li, Q.; Guo, X.; Huang, X.; Huang, Q. Advanced glycation end products induce moesin phosphorylation in murine brain endothelium. *Brain Res.* **2011**, *1373*, 1–10. [CrossRef]
25. Kim, K.S.; Itabashi, H.; Gemski, P.; Sadoff, J.; Warren, R.L.; Cross, A.S. The K1 capsule is the critical determinant in the development of Escherichia coli meningitis in the rat. *J. Clin. Investig.* **1992**, *90*, 897–905. [CrossRef]
26. Doran, K.S.; Fulde, M.; Gratz, N.; Kim, B.J.; Nau, R.; Prasadarao, N.; Schubert-Unkmeir, A.; Tuomanen, E.I.; Valentin-Weigand, P. Host-pathogen interactions in bacterial meningitis. *Acta Neuropathol.* **2016**, *131*, 185–209. [CrossRef]
27. Kim, K.S. Mechanisms of microbial traversal of the blood-brain barrier. *Nat. Rev. Microbiol.* **2008**, *6*, 625–634. [CrossRef]
28. Liu, W.-T.; Lv, Y.-J.; Yang, R.-C.; Fu, J.-Y.; Liu, L.; Wang, H.; Cao, Q.; Tan, C.; Chen, H.-C.; Wang, X.-R. New insights into meningitic Escherichia coli infection of brain microvascular endothelial cells from quantitative proteomics analysis. *J. Neuroinflamm.* **2018**, *15*, 291. [CrossRef]
29. Sharma, H.S.; Pontén, E.; Gordh, T.; Eriksson, P.; Fredriksson, A.; Sharma, A. Propofol promotes blood-brain barrier breakdown and heat shock protein (HSP 72 kd) activation in the developing mouse brain. *CNS Neurol. Disord. Drug Targets* **2014**, *13*, 1595–1603. [CrossRef]
30. Doronzio, A.; Lanni, F.; Ayrian, E.; Zhang, Y.P.; Bilotta, F.; Rosa, G. Postoperative delirium after anestesia with propofol, sevoflurane or desflurane: The Pinocchio trial. Interim analysis of safety and preliminary results: 7AP3-6. *Eur. J. Anaesthesiol.* **2013**, *30*, 108–109. [CrossRef]
31. Ishii, K.; Akiyama, D.; Hara, K.; Makita, T.; Sumikawa, K. Influence of general anesthetics on the incidence of postoperative delirium in the elderly. *Masui* **2011**, *60*, 856–858.

32. Ishii, K.; Makita, T.; Yamashita, H.; Matsunaga, S.; Akiyama, D.; Toba, K.; Hara, K.; Sumikawa, K.; Hara, T. Total intravenous anesthesia with propofol is associated with a lower rate of postoperative delirium in comparison with sevoflurane anesthesia in elderly patients. *J. Clin. Anesth.* **2016**, *33*, 428–431. [CrossRef] [PubMed]
33. Weber, V.; Bork, K.; Horstkorte, R.; Olzscha, H. Analyzing the Permeability of the Blood-Brain Barrier by Microbial Traversal through Microvascular Endothelial Cells. *J. Vis. Exp.* **2020**. [CrossRef] [PubMed]
34. Stins, M.F.; Badger, J.; Sik Kim, K. Bacterial invasion and transcytosis in transfected human brain microvascular endothelial cells. *Microb. Pathog.* **2001**, *30*, 19–28. [CrossRef] [PubMed]
35. Dhananjayan, K.; Irrgang, F.; Raju, R.; Harman, D.G.; Moran, C.; Srikanth, V.; Münch, G. Determination of glyoxal and methylglyoxal in serum by UHPLC coupled with fluorescence detection. *Anal. Biochem.* **2019**, *573*, 51–66. [CrossRef]
36. Scheffler, J.; Bork, K.; Bezold, V.; Rosenstock, P.; Gnanapragassam, V.S.; Horstkorte, R. Ascorbic acid leads to glycation and interferes with neurite outgrowth. *Exp. Gerontol.* **2019**, *117*, 25–30. [CrossRef]
37. Wessén, A.; Persson, P.M.; Nilsson, A.; Hartvig, P. Concentration-effect relationships of propofol after total intravenous anesthesia. *Anesth. Analg.* **1993**, *77*, 1000–1007.
38. Takizawa, E.; Hiraoka, H.; Takizawa, D.; Goto, F. Changes in the effect of propofol in response to altered plasma protein binding during normothermic cardiopulmonary bypass. *BJA Br. J. Anaesth.* **2005**, *96*, 179–185. [CrossRef]
39. Minami, K.; Körner, M.M.; Vyska, K.; Kleesiek, K.; Knobl, H.; Körfer, R. Effects of pulsatile perfusion on plasma catecholamine levels and hemodynamics during and after cardiac operations with cardiopulmonary bypass. *J. Thorac. Cardiovasc. Surg.* **1990**, *99*, 82–91. [CrossRef]
40. Bhardwaj, A.; Brannan, T.; Martinez-Tica, J.; Weinberger, J. Ischemia in the dorsal hippocampus is associated with acute extracellular release of dopamine and norepinephrine. *J. Neural. Transm. Gen. Sect.* **1990**, *80*, 195–201. [CrossRef]
41. Yasuda, Y.; Nishikimi, M.; Nishida, K.; Takahashi, K.; Numaguchi, A.; Higashi, M.; Matsui, S.; Matsuda, N. Relationship Between Serum Norepinephrine Levels at ICU Admission and the Risk of ICU-Acquired Delirium: Secondary Analysis of the Melatonin Evaluation of Lowered Inflammation of ICU Trial. *Crit. Care Explor.* **2020**, *2*, e0082. [CrossRef] [PubMed]
42. Windmann, V.; Spies, C.; Knaak, C.; Wollersheim, T.; Piper, S.; Vorderwülbecke, G.; Kurpanik, M.; Kuenz, S.; Lachmann, G. Intraoperative hyperglycemia increases the incidence of postoperative delirium. *Minerva Anestesiol.* **2019**, *85*. [CrossRef] [PubMed]
43. Rao, G.G.; Rao, V.N. Ascorbic acid as a reducing agent in quantitative analysis. *Fresenius Z. Anal. Chem.* **1955**, *147*, 338–347. [CrossRef]
44. Krone, C.A.; Ely, J.T. Ascorbic acid, glycation, glycohemoglobin and aging. *Med. Hypotheses* **2004**, *62*, 275–279. [CrossRef]
45. Roy, J.; Galano, J.M.; Durand, T.; Le Guennec, J.Y.; Lee, J.C. Physiological role of reactive oxygen species as promoters of natural defenses. *FASEB J.* **2017**, *31*, 3729–3745. [CrossRef]
46. Frei, B.; England, L.; Ames, B.N. Ascorbate is an outstanding antioxidant in human blood plasma. *Proc. Natl. Acad. Sci. USA* **1989**, *86*, 6377–6381. [CrossRef]
47. Hill, A.; Wendt, S.; Benstoem, C.; Neubauer, C.; Meybohm, P.; Langlois, P.; Adhikari, N.K.; Heyland, D.K.; Stoppe, C. Vitamin C to Improve Organ Dysfunction in Cardiac Surgery Patients-Review and Pragmatic Approach. *Nutrients* **2018**, *10*, 974. [CrossRef]
48. Volpe, C.M.O.; Villar-Delfino, P.H.; dos Anjos, P.M.F.; Nogueira-Machado, J.A. Cellular death, reactive oxygen species (ROS) and diabetic complications. *Cell Death Dis.* **2018**, *9*, 119. [CrossRef]
49. Vinson, J.; Howard, T. Inhibition of protein glycation and advanced glycation end products by ascorbic acid and other vitamins and nutrients. *J. Nutr. Biochem.* **1996**, *7*, 659–663. [CrossRef]

proteomes

MDPI

Article

Disturbance of Key Cellular Subproteomes upon Propofol Treatment Is Associated with Increased Permeability of the Blood-Brain Barrier

Timo Längrich [1], Kaya Bork [1], Rüdiger Horstkorte [1], Veronika Weber [1], Britt Hofmann [2], Matt Fuszard [3] and Heidi Olzscha [1,4,*]

[1] Institut für Physiologische Chemie, Martin-Luther-Universität Halle-Wittenberg, Hollystr. 1, 06114 Halle (Saale), Germany
[2] Klinik und Poliklinik für Herzchirurgie, Universitätsklinikum Halle (Saale), Ernst-Grube-Str. 20, 06120 Halle (Saale), Germany
[3] Core Facility—Proteomic Mass Spectrometry, Proteinzentrum Charles Tanford, Kurt-Mothes-Straße 3a, 06120 Halle (Saale), Germany
[4] Medical School Hamburg MSH, University of Applied Sciences and Medical University, Institute of Molecular Medicine, Am Sandtorkai 76, 20457 Hamburg, Germany
* Correspondence: heidi.olzscha@medicalschool-hamburg.de

Abstract: Background: Propofol is a short-acting anesthetic, which is often used for induction and maintenance of general anesthesia, sedation for mechanically ventilated adults and procedural sedation. Several side effects of propofol are known and a substantial number of patients suffer from post-operative delirium after propofol application. In this study, we analyzed the effect of propofol on the function and protein expression profile on a proteome-wide scale. Methods: We cultured human brain microvascular endothelial cells in absence and presence of propofol and analyzed the permeability of the blood-brain barrier (BBB) by fluorescein passage and protein abundance on a proteome-wide scale by mass spectrometry. Results: Propofol interfered with the function of the blood-brain barrier. This was not due to decreased adhesion of propofol-treated human brain microvascular endothelial cells. The proteomic analysis revealed that some key pathways in these cells were disturbed, such as oxygen metabolism, DNA damage recognition and response to stress. Conclusions: Propofol has strong effects on protein expression which could explain several side effects of propofol.

Keywords: anesthetics; blood-brain barrier; DNA damage response; drug effect; human brain microvascular endothelial cells; metabolic stress; propofol; proteome; quantitative proteomics; reactive oxygen species (ROS)

check for updates

Citation: Längrich, T.; Bork, K.; Horstkorte, R.; Weber, V.; Hofmann, B.; Fuszard, M.; Olzscha, H. Disturbance of Key Cellular Subproteomes upon Propofol Treatment Is Associated with Increased Permeability of the Blood-Brain Barrier. *Proteomes* **2022**, *10*, 28. https://doi.org/10.3390/proteomes10030028

Academic Editors: Yannis Karamanos and Gwenael Pottiez

Received: 24 June 2022
Accepted: 3 August 2022
Published: 15 August 2022

Publisher's Note: MDPI stays neutral with regard to jurisdictional claims in published maps and institutional affiliations.

1. Introduction

The blood-brain barrier (BBB) is a semipermeable barrier that separates the peripheral blood from the brain parenchyma. It ensures that both endogenous substances and cells as well as exogenous substances and cells such as drugs or pathogens are prevented from entering the brain [1]. There are mainly three cell types that are the building blocks of the human BBB: the brain microvascular endothelial cells (BMECs), pericytes and astrocytes [2]. The BMECs are of particular importance for building a tight BBB, as they are pivotal in providing tight junctions and adherens junctions [3,4]. It has been reported that the rate of transcytosis in BMECs is comparably low, which leads to a tight and controlled BBB [5]. These polarized cells contribute to a tight paracellular and transcellular barrier which restricts the entry of the beforementioned components [6]. However, small lipophilic molecules can pass the BBB by the process of diffusion, whereas many larger hydrophilic molecules cannot pass this barrier and need to be transported via selectively expressed transport systems [7]. Transport systems ensure that molecules can be transported into the

brain and waste products can be removed, especially, the so-called nutrient transporters help in transporting nutrients into the central nervous system (CNS) [8]. Since the brain is one of the organs with the highest energy-consumption, it is conceivable that nutrients and oxygen should not be the limiting factor. This is also reflected in the BMECs, as they express more mitochondria than comparable endothelial cells [9]. On the one hand, this can help the cells to fulfill their tasks in transporting and producing a sufficient concentration of molecules to maintain the barrier. On the other hand, the cells need a functioning system to remove excessive metabolites and even toxic products including reactive oxygen species (ROS), and a dysfunction of these systems could contribute to an increased permeability of the BBB [10].

Many pathological conditions are known to affect the integrity of the BBB, and some of them have been found to be associated with a disturbed oxygen metabolism. For instance, it has been shown that ROS and a disturbed oxygen metabolism affecting the BBB can deteriorate some neurodegenerative disorders such as Alzheimer's disease (AD) and amyotrophic lateral sclerosis (ALS) [11,12]. However, it is still unclear, whether these phenomena are consequent reactions or causal in the etiology of these diseases. It is also still unclear, whether the effects of a disturbed oxygen metabolism are reversible and whether they could be treated.

Other than neurodegenerative disorders, there are other diseases known to be affected by decreased integrity of the BBB, for instance septic encephalopathy. It has been demonstrated that this condition can be associated with elevated protein levels in the cerebrospinal fluid and an increased uptake of different forms of iron oxide [13]. These phenomena are accompanied with increased permeability of the BBB and altered signal transduction in BMECs [14]. Cerebral ischemia is another pathologic condition which can lead to an increase in the permeability of the BBB [15,16], underpinning the hypothesis that altered oxygen levels and ROS can affect the integrity of the BBB. In the same vein, it has been reported that cerebral edema, which can occur after an ischemic stroke, can also have a significant impact on the tightness of the BBB, as the swelling of the cerebral tissue by the edema can culminate in an ischemic injury [17]. Other diseases which are also associated with an increased permeability of the BBB, are for instance meningitis and sepsis [18]. There are also indications that sepsis can be accompanied with post-operative delirium (POD), which can also contribute to the disruption of the BBB [19]. In the case of septic encephalopathy, patients display increased protein levels in the cerebrospinal fluid [20] and increased uptake of marked colloidal iron oxide has been reported in an animal model [21].

There exist several studies indicating that anesthesia can affect the BBB. One particular example we previously investigated was the non-volatile anesthetic propofol [22]. Propofol is a phenolic derivative and is considered one of the more favorable intravenous anesthetics due to its rapid onset of effect, short plasma half-life and its low accumulation in tissues [23]. Propofol is used for clinical anesthesia induction (4–6 μg/mL), maintenance of anesthesia and sedation (1–3 μg/mL) [24–26]. For instance, a concentration of 2.5 to 4 μg/mL is used during maintenance of anesthesia of normothermic cardiopulmonary bypass [27]. Other than the desired sedative effects, it causes hemodynamic [28], respiratory [29], neurological [30], endocrine [31] and immunogenic [32] effects. Propofol is a lipophilic compound, and can therefore rapidly cross the BBB. This also implies that propofol has to be dissolved in a lipophilic vehicle. Usually, it is formulated as an emulsion containing propofol, soybean oil (100 mg/mL), glycerol (22.5 mg/mL), egg lecithin (12 mg/mL) and disodium edetate (0.005%) with sodium hydroxide to adjust the pH to 7–8.5. This also implies that some, but not all of the side effects of propofol, can be explained by the accessory components in the emulsion, such as hyperlipidemia and also indicates the need for antimicrobial agents [33]. It has been previously shown that propofol can substantially reduce ischemia and reperfusion in particular by a decrease of reactive oxygen species (ROS), reduction of free radicals, helping in protection of the cell membrane and mitochondrial function from lipid peroxidation and a prevention of apoptosis [34–36].

It has been hypothesized that these mechanisms could contribute to an altered permeability of the BBB. However, there exist also reports showing that anesthetics including propofol did not alter the permeability of the BBB or even reduced an increased permeability during a 2% hypoxia [37]. In addition, there are indications that propofol may act in protecting DNA damage, including induced double strand breaks. Especially the ROS-induced DNA damage has been shown to be reduced by propofol treatment [38].

Considering our previous results and the aforementioned literature, we aimed with this current study to elucidate the effects of propofol on the BBB and systematically analyze changes in the proteome. With a previously established cellular model system [39], we demonstrated that propofol, but not its lipophilic vehicle formulation, leads to an increased permeability of the BBB model, whereas the cellular adhesion remained unchanged compared to the untreated control. Quantitative proteomic analysis by LC-MS/MS of the protein levels upon treatment with propofol revealed profound changes in biological processes (GO terms; [40,41]) such as oxygen transport, hydrogen peroxide processes, response to stress and DNA-damage recognition. We confirmed these results by biochemical means and could give evidence that the levels of representative proteins of these processes were altered. We could therefore give an explanation on a proteomic level for the previous observed effects of propofol on altered oxygen metabolisms, including the role of iron, DNA damage response (DDR) and a potential reversal of DNA damage. In addition, it could also explain some of the beforementioned long-term adverse effects. Since we clearly distinguished with our experiments between propofol itself and the lipidous emulsion, our results can give guidance on how to reduce the adverse effects.

2. Materials and Methods

2.1. Cells and Cell Culture

Transfected human brain microvascular endothelial cells (THBMEC), provided by MF Stins (Los Angeles, CA, USA), were used as model for BBB endothelial cells. DMEM/F12 medium (Thermo Fisher Scientific, Waltham, MA, USA) supplemented with 100 mg/L penicillin and 100 mg/L streptomycin (Thermo Fisher Scientific), 2 mM L-glutamine (Thermo Fisher Scientific) and 10% heat-inactivated fetal calf serum (GE Healthcare, Little Chalfont, UK) was used for cultivation at 37 °C in a humified cell culture incubator. Cells were passaged every 2–3 days. Therefore, THBMECs were detached with 1% Trypsin/EDTA (Thermo Fisher Scientific) and pelleted at 210 g for 5 min. A more detailed description of the method is given in [39].

2.2. Measurement of Fluorescein Passage through the BBB

Testing the effect of propofol treatment on the permeability of the human BBB was performed by an endothelial cell culture model, which mimics a tight BBB model with human brain microvascular endothelial cells (THBMEC) [42]. THBMECs were grown on 12-well filters with 3.0-µm pore size (ThinCerts, Greiner Bio-One, Kremsmünster, Austria) for 14 days until they form a confluent layer. Firstly, filters were coated with a mixture of 10 µg/mL collagen IV and 10 µg/mL fibronectin (Sigma-Aldrich, Saint Louis, MO, USA) for 24 h. Incubation of the cells was performed using a cell culture incubator with 5% CO_2 atmosphere at 37 °C. DMEM/F-12 medium was changed every 2 to 3 days in the upper and lower chamber. Propofol (Sigma-Aldrich) was dissolved in lipid mixture (SMOFlipid, FreseniusKabi, Bad Homburg, Germany). On day 14 of growth, propofol was added to serum free medium in the upper chamber to a final concentration of 3 µg/mL, an equal amount of the lipid mixture served as a control. After 24 h of treatment, the medium was removed, cells were washed two times with PBS and serum free medium without phenol red was given into both chambers. Fluorescein was added to the upper chamber, with a final concentration of 10 µg/mL. After an incubation time of 180 min, aliquots were taken from lower chamber and fluorescence intensity was measured (Clariostar, BMG Labtech GmbH, Ortenberg, Deutschland) at a wavelength of 535 nm (excitation: 488 nm).

A calibration curve was produced by using a dilution series with known concentration of fluorescein (2 ng/mL to 1 mg/mL).

2.3. Real Time Cell Adhesion Assay

xCelligence RTCA DP® in combination with E-Plates® (OMNI Life Science, Bremen, Germany) was used for time-dependent measurement. On a first step E-Plates® were coated with 10 µg/mL collagen IV and 10 µg/mL fibronectin for 72 h. Plates were washed twice with PBS and then blocked with 0.5% bovine serum albumin (Carl Roth, Karlsruhe, Germany) in PBS for 30 min at 37 °C. Cells were detached with 1% Trypsin/EDTA and counted while wells were equilibrated for 15 min with 50 µL medium at 37 °C. After incubation time, the plates were set into RTCA DP® and blank was measured. Afterwards 2500 cells were seeded in every well and propofol was given directly into medium, untreated cells and cells treated with lipid served as a control. Cell index was measured automatically every 15 min.

2.4. Preparation of Cell Extracts

After incubation, treated and control cells were removed from the surface by scraping and washed twice in ice cold PBS. Lysis buffer was prepared by supplementing solubilization buffer (50 mM Tris pH = 7.4, 150 mM NaCl, 1% Triton X-100, 1% SDS (sodium dodecyl sulfate), 1 mM EDTA (ethylenediaminetetraacetic acid)) with 0.2% PIC (protease inhibitor cocktail), 0.1% PMSF (phenylmethylsulfonylfluoride), 0.05% Mg132, 1% Sodium orthovanadate, each 1% phosphatase inhibitor cocktail II and III, 5 µM SAHA (suberoylanilide hydroxamic acid) and 400 µM NEM (*N*-ethylmaleimide). Protein concentration was measured using BCA (bicinchoninic acid assay, Thermo Scientific Fisher) following the manufacturer's instructions.

2.5. Mass Spectrometry

2.5.1. Sample Preparation

First, 10 µg of protein from each sample were aliquoted and the remaining sample stored at −20 °C. Samples were then prepared for mass spectrometry analysis with the USP3 protocol as described [43]. In brief, 1 µL of pre-prepared Sera-Mag speed beads were added to each sample and vortexed. Acetonitrile (ACN) was added to 70% and the mixture incubated for 20 min at RT in a thermo mixer at 400 rpm to allow proteins to adsorb to the beads. Samples were placed on a magnetic rack for 2 min and the supernatant was discarded. Samples were subsequently washed three times on-bead with 70% ethanol and finally with pure ACN. After lyophilizing the beads to remove ACN, samples were re-suspended in 50 mM Ammonium Bicarbonate and reduced with 10 nM DTT at 80 °C for 15 min. After cooling samples were alkylated with 20 mM CAA for half an hour at room temperature in the dark. LysC/trypsin was added at a ratio of 1:50 enzyme:substrate and incubated overnight at 37 °C. Samples were then placed on a magnetic rack for 2 min and the supernatant with peptides were removed for C18 spin column clean up (Pierce™ C18 Spin Tips, Thermo Scientific #84850) as recommended by the manufacturer.

2.5.2. LC-MSMS

Approximately 200 ng of peptides for each sample and replicate were initially trapped (PepMap100 5 µm, 3 × 5 mm Thermo Scientific #160454) and separated on a Waters M-Class C18 25 cm analytical column (Acquity UPLC® M-Class HSS T3 1.8 µm 75 µm × 250 mm, Waters #18600) over 180 min with an increasing gradient of ACN (3–22%) at 240 nL/min before being injected in to a Thermo Scientific Orbitrap Exploris 480 mass spectrometer. Peptides were ionized in positive mode with 1800 V and a transfer capillary temperature of 300 °C. Samples were subjected to further separation with FAIMS pro with 3 compensation voltages (CVs: −40, −55, −65), resulting in 3 separate MS experiments within one data file. Each experiment had the following settings: MS resolution of 120,000 at 00 m/z, a scan range of 350–1400 m/z, MS AGC target of 300% for max IT of 50 ms; MSMS of all the most

intense peaks for a total cycle time of 1 s with the following settings: Isolation window of 2 m/z normalized collision energy of 30%, resolution of 15 000 with an AGC target of 100% and a max 30 ms IT. Every fragmented precursor within +/−10 ppm was immediately excluded from reanalysis for 45 s.

2.5.3. Data Analysis

Raw data files were analyzed within Proteome Discoverer 2.4.0.305 following a LFQ quantification workflow. Searches were performed against the Human database (accessed 7 July 2020—Uniprot proteome UP000005640) with decoys using Sequest HT with a precursor tolerance of 10 ppm and a fragment mass tolerance of 0.02 Da, trypsin as a cleavage agent with 2 missed cleavages considered. Carbamidomethylation of cysteines was set as a static modification, and the following dynamic modifications were investigated: oxidation (M), acetylation (K), phosphorylation (S, T, Y), ubiquitination (GG on K), as well as N-terminal protein modifications of acetylation, met-loss and acetylation + met-loss. IDs were filtered with Percolator at a strict FDR of 0.01. Precursor ion quantification was performed with unique and razor peptides with Top N of 3. Precursor abundance was based upon intensity and normalized over total peptide amount. Quantification was based on ratios of lipid:control and propofol:control where pairwise ratios were calculated and *t*-tests were used for hypothesis testing [43].

The mass spectrometry proteomics data have been deposited to the ProteomeXchange Consortium via the PRIDE [44] partner repository with the dataset identifier PXD033856 and 10.6019/PXD033856.

2.6. Immunoblotting

Cell lysates were supplemented with SDS-sample buffer (100 mL buffer containing 12.5% SDS, 0.3 M Tris, 50 mL glycerin, bromophenol blue at pH 6.8 and 1:10 DTT to buffer) and heated at 95 °C for 10 min. Then, 40 µg of each sample were applied on a 12% acrylamide gel and separated by SDS-PAGE. Afterwards proteins were transferred to a nitrocellulose membrane for 1 h 15 min in blotting buffer with a constant amperage of 300 mA. To avoid overheating, blot chamber (VWR, Radnor, PA, USA) was cooled down during the blotting process. To prove successful protein transfer staining with ponceau red solution containing 0.1% ponceau S (Carl Roth, Karlsruhe, Germany), 3% trichloroacetic acid and 3% sulfosalicylic acid was applied. Before incubating the membrane with the primary antibodies, it was blocked with 5% milk in 1 × TBS supplemented with 0.05% Tween-20 (TBS-T) at room temperature for 1 h. Incubation with primary antibodies was performed overnight at 4 °C. Histone H2AX was detected by rabbit monoclonal Anti-Histone H2AX antibody (ab229914, Abcam, Cambridge CB2 0AX, UK) at a 1:1000 dilution. FTH1 was detected using FTH1 Rabbit monoclonal antibody (CST 4393, Cell Signaling Technologies, Danvers, MA, USA) at a dilution of 1:1000. The next day the membrane was washed three times with TBS-T for 15 min and then incubated with HRP-conjugated goat-anti-rabbit-antibody (ab6721, Abcam), diluted 1:20,000, at room temperature for 1 h. Antibody binding to specific proteins were detected by using Luminata Forte Western HRP-Substrate (Merck Millipore, Billerica, MA, USA) and signals were visualized using the ChemiDoc MP Imaging System (BioRad, Hercules, CA, USA). Analysis was performed by using the associated ImageLab software (BioRad). For normalization of band intensity of the Western blot Ponceau S staining served as the loading control. Comparison and *p*-value determination of two samples in the quantitated Western blots was performed by using a paired student's *t*-test.

3. Results

In order to quantify the effects of propofol on the permeability of the BBB for compounds from the blood, we used our recently established BBB-model, which takes advantage of human brain endothelial cells (THBMEC) [39]. These cells were grown on filters until confluence and prevent diffusion of molecules from the upper to the lower side of the filter.

3.1. Propofol Increases the Permeability of the BBB

Before studying the permeability of the BBB after application of propofol, we analyzed the cell viability of THBMEC cells in the presence of propofol with 3 µg/mL, which is a commonly used concentration in surgery, and found that the cell viability was not affected by propofol (data not shown and in [22]). The effect of propofol on the permeability of THBMECs was further analyzed. Treatment with 3 µg/mL propofol resulted in an increase of the permeability of the endothelial cells (Figure 1), whereas the lipid solution, in which propofol is dissolved, had no effect.

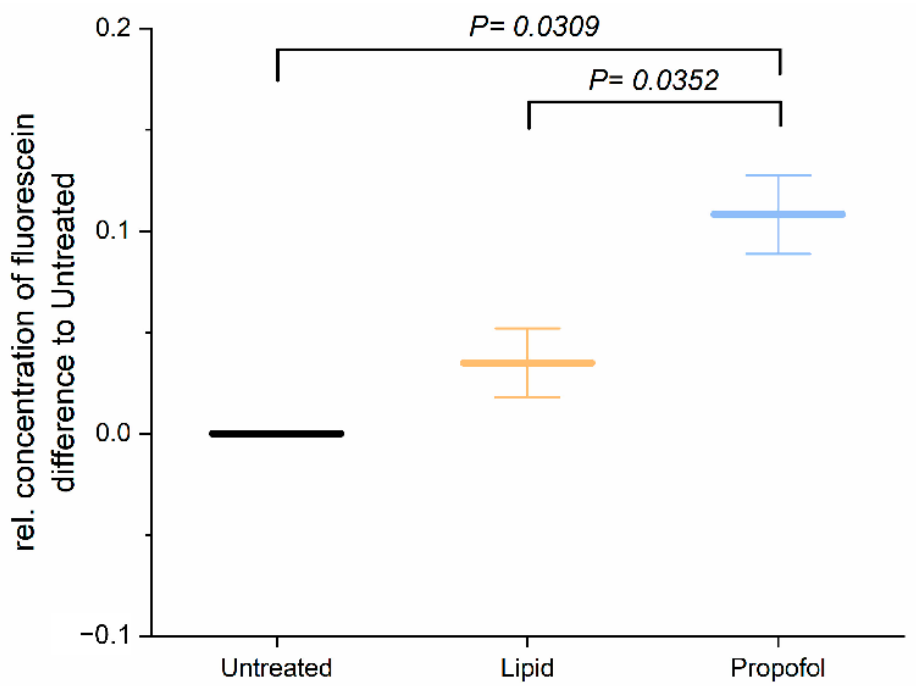

Figure 1. Cells were treated with 3 µg/mL propofol, dissolved in lipid solution, for 24 h. Lipid treatment and untreated cells served as control. Fluorescein was applied to the upper chamber and the concentration in lower chamber was quantified after 1 h. The bar chart represents mean of relative concentration of fluorescein ± SD (n = 3).

Since tightness and permeability of the BBB rely mainly on cell adhesion, we analyzed next the adhesion of THBMECs on the surface. In order to determine the cellular adhesion, we performed a real-time cell adhesion assay. The time course of one representative experiment is shown in Figure 2A. There was no significant difference in adhesion of THBMECs in the absence or presence of propofol over 3 h of adhesion. Figure 2B shows the relative mean adhesion of three independent experiments after 3 h.

3.2. Propofol Interferes with Protein Expression of the BBB

We then asked the question: why propofol interferes with the permeability of the BBB without interfering neither cell viability nor cell adhesion? To answer this question, we analyzed the protein abundance of THBMECs cultured in the absence or presence of propofol by quantitative mass spectrometry. We were able to identify 6903 protein groups across 3 conditions (n (replicates per condition) = 3). Of these, 5440 proteins were quantifiable (FDR < 0.01; #unique peptides ≥ 2, n = 9). The volcano plots of the differentially abundant proteins are given in Figure 3. Lipid vs. control saw 23 proteins that were differentially abundant (17 down, 6 up), propofol vs. control had 22 proteins (12 down, 10 up) and propofol vs. lipid had 24 (5 down, 19 up) (Supplementary Tables S1–S4, Supplementary Figure S1).

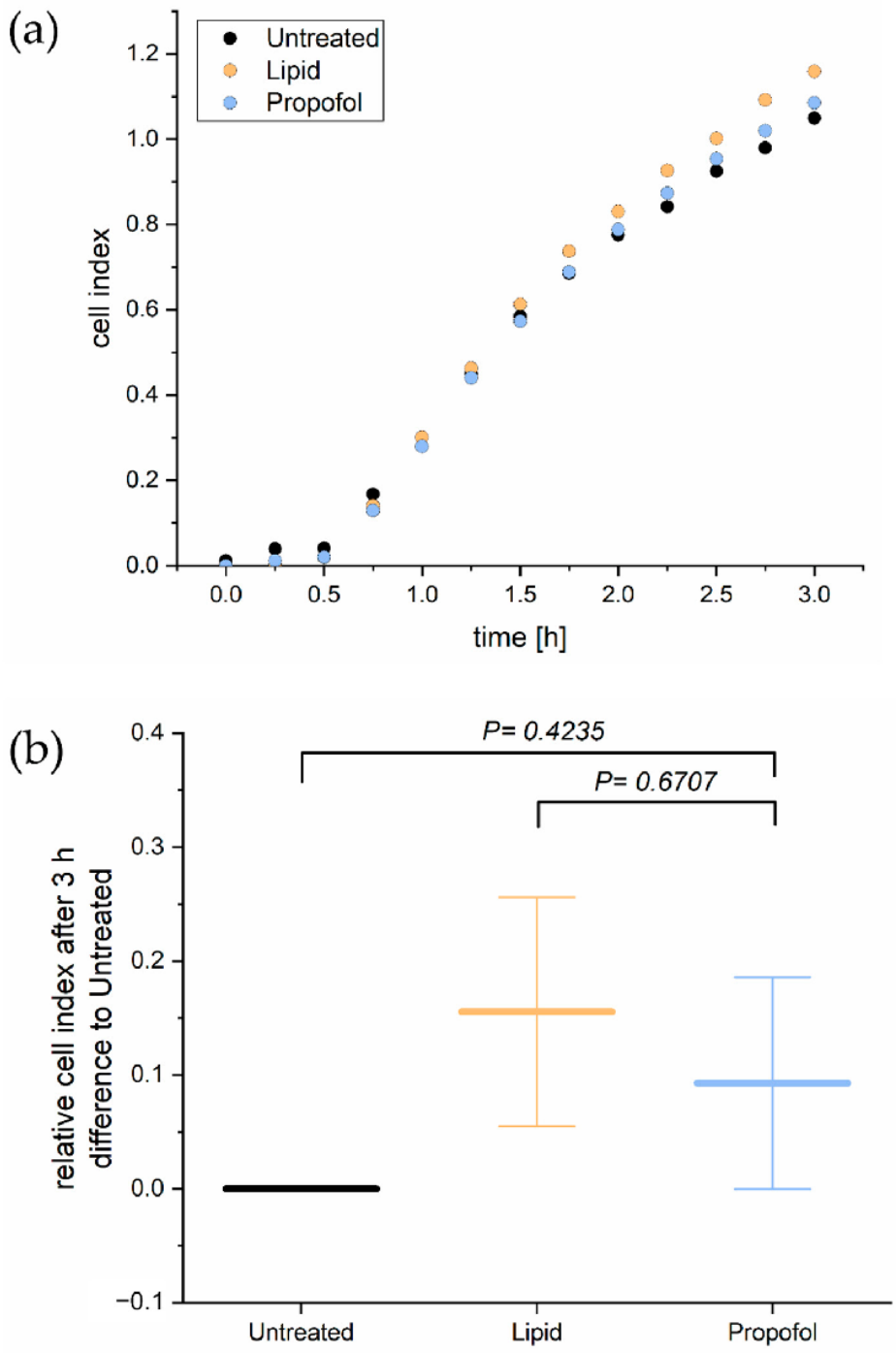

Figure 2. Real time cell adhesion assay. Cells were treated with 3 µg/mL propofol. Cell adhesion was measured every 15 min for 3 h (**a**). The bar chart represents differences of the mean cell index compared to propofol treated cells and cells treated with the only the lipid vehicle ± SD after 3 h (**b**), ($n = 3$).

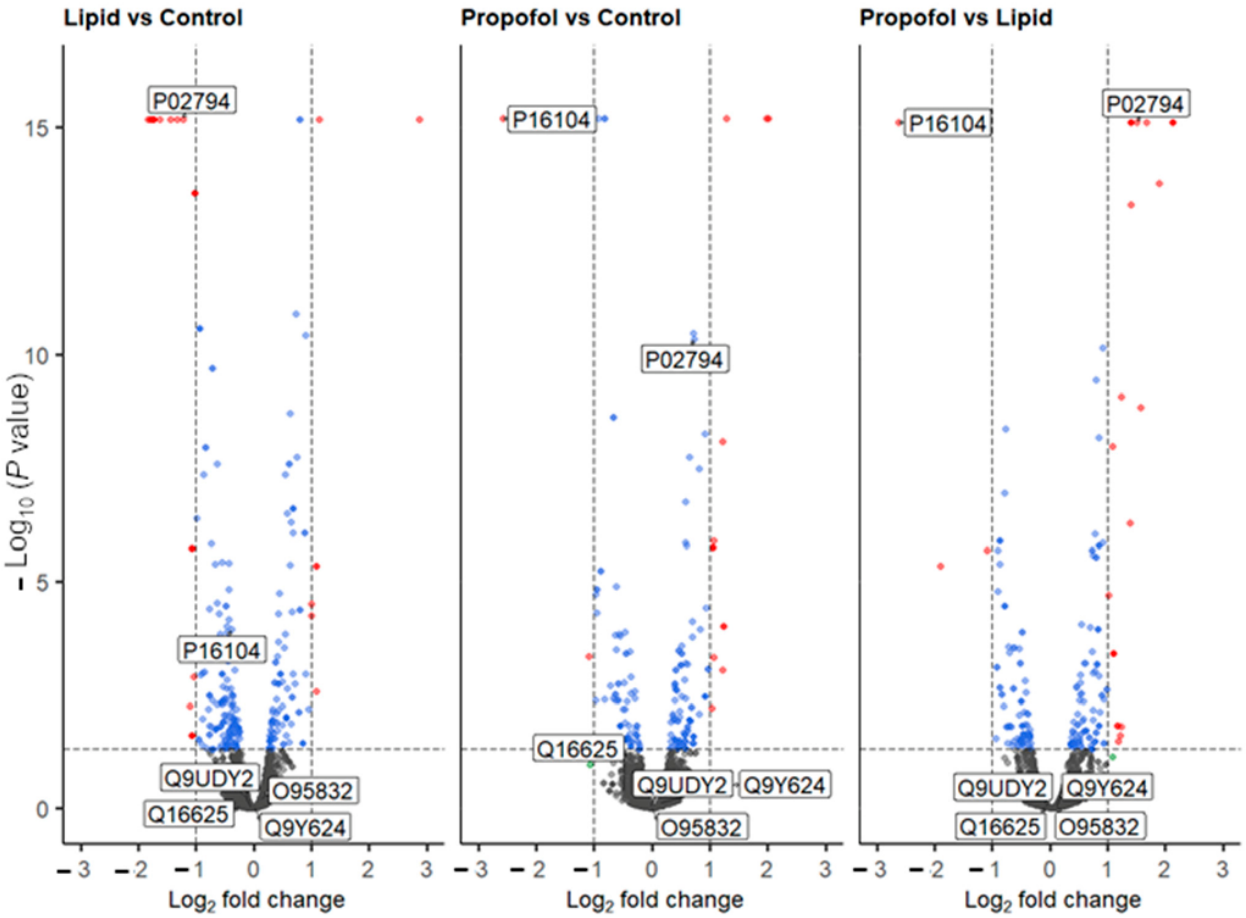

Figure 3. Volcano plot of all quantified proteins from the three different comparative experiments. Proteins that are up- or down-regulated are shown in red. Labels are Uniprot codes, whereby P16104 has the gene name H2AFX (protein name H2AX), and P02794 is FTH1. Dotted lines represent significant differences from control and is given by $p < 0.05$, and fold change (log2) > 2. Blue dots represent data points that have passed the p value threshold and the red dots are data points that have passed both the p value and fold change thresholds listed above.

Based on the MS data, we analyzed the protein levels of two specific proteins in more detail, namely the histone H2AX (P16104, gene name *H2AFX*, Figure 3), which was found to be down-regulated in the MS analysis after propofol vs. control (FC = −2.58, $p < 0.001$) and propofol vs. lipid (FC = −2.62, $p < 0.001$) (but not lipid vs. control, but was mildly depressed (FC = −0.39, $p < 0.001$)) and the heavy chain subunit FTH1 (P02794, Figure 3) of ferritin, which was significantly up-regulated upon propofol vs. lipid (FC = 1.5, $p < 0.001$), but not significantly different in propofol vs. control (FC = 0.72, $p < 0.001$) and down-regulated in lipid vs. control (FC = −1.23, $p < 0.001$).

We also performed a cluster analysis by String implemented in Cytoscape in order to find interactions between differently expressed proteins. Up- and down-regulated proteins form different clusters are depicted in Figure 4. Looking at the enriched terms of GO biological processes, oxygen transport and response to stress are found in up-regulated proteins, while down-regulated proteins are associated with chromosome organization.

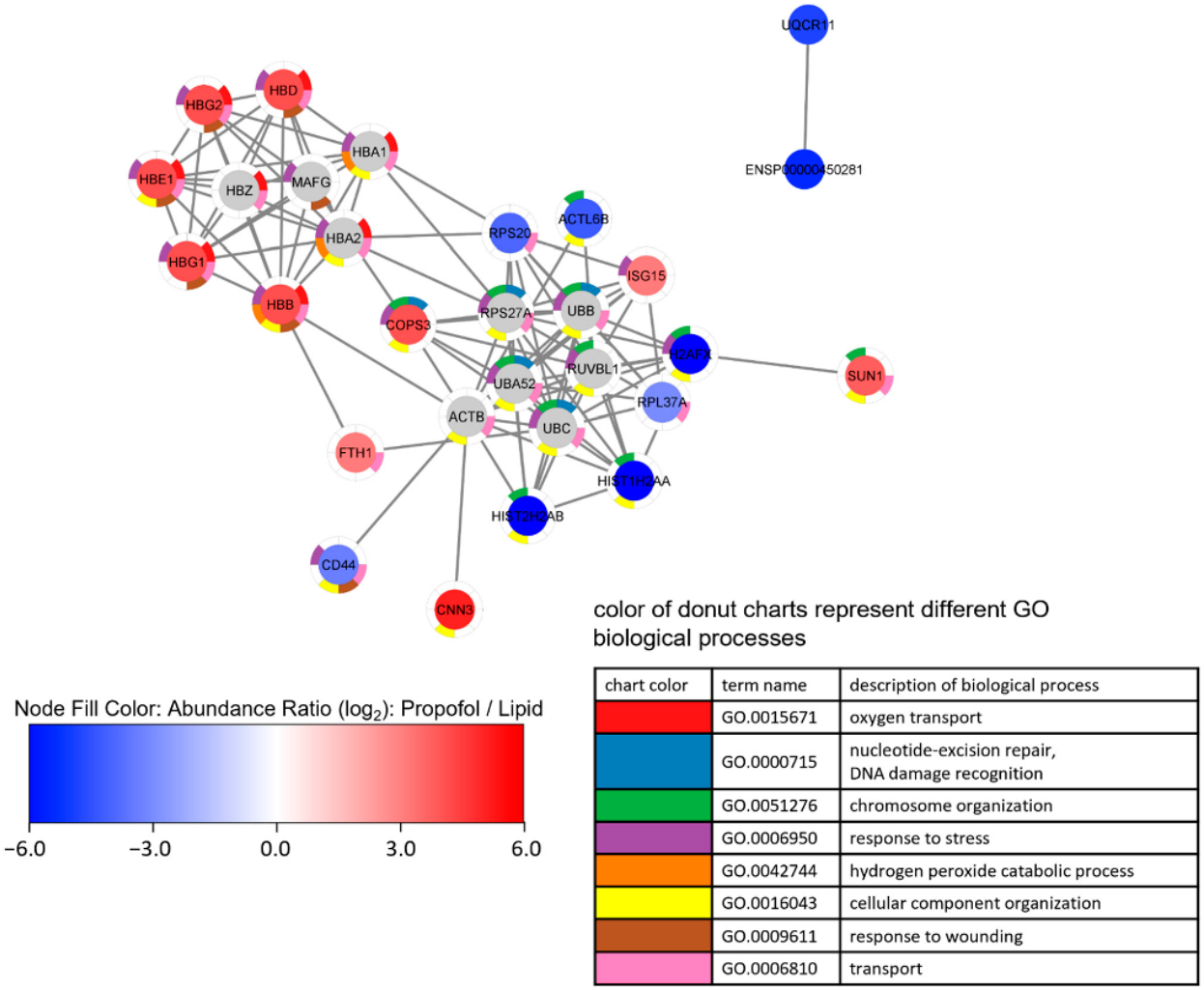

chart color	term name	description of biological process
	GO.0015671	oxygen transport
	GO.0000715	nucleotide-excision repair, DNA damage recognition
	GO.0051276	chromosome organization
	GO.0006950	response to stress
	GO.0042744	hydrogen peroxide catabolic process
	GO.0016043	cellular component organization
	GO.0009611	response to wounding
	GO.0006810	transport

Figure 4. Network analysis of a proteome network after propofol treatment. Cells were treated with 3 µg/mL propofol for 12 h, lipid treatment served as a control. Total protein was isolated and analyzed by mass spectrometry (n = 3). Proteins are filtered according following parameter: (1) 1.5-fold increase or decrease in abundance ratio ($\log_2$)—propofol vs. lipid; (2) coverage $\geq$ 5%; (3) protein found in every sample.

Proteins were clustered by String via Cytoscape using up to 10 interactors, followed by an enrichment analysis. Node fill color represents abundance ratio ($\log_2$)—propofol vs. lipid, interactors added by String are colored grey. The donut chart represents the eight most significant terms of GO biological processes found in the enrichment analysis, which is reflected in the legend. Proteins without annotated interactions are not shown.

Given these observations in the MS experiments, and given the importance of the aforementioned proteins to the processes in Figure 4, we validated the changing protein levels of these two proteins by Western blot analysis as shown in Figure 5. We found a substantial reduction of H2AX protein expression compared to control (Figure 5A) and a slight increase in FTH1 protein expression (Figure 5B), which correlates with the data obtained by MS. The comparative differences of both proteins in expression are clearly shown in propofol vs. lipid (Figure 4) and the Western blots.

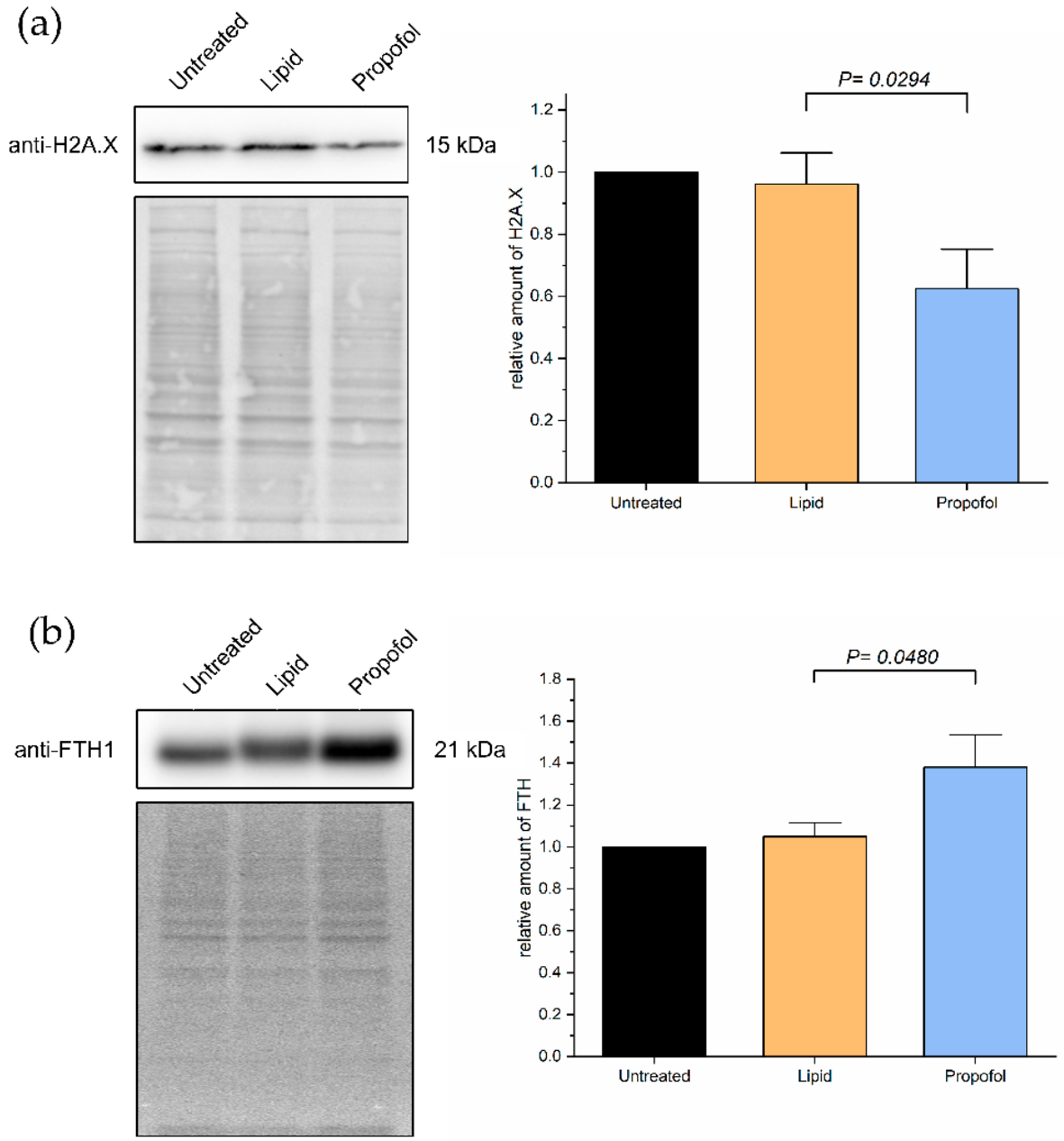

Figure 5. Cells were treated with 3 µg/mL propofol for 48 h, untreated cells and lipid treatment served as control. Afterwards, total protein was isolated and separated using SDS-PAGE. Expression of proteins was detected via immuno-blotting using anti-H2AX-antibody (**a**) and anti-FTH-antibody (**b**) ($n = 4$). Ponceau S served as a loading control. Bar chart represents mean of amount of target protein ± SD relative to untreated cells.

4. Discussion

In this study, we could demonstrate that propofol affects the blood-brain-barrier on human endothelial cells. Importantly, it directly reduces its function by increasing the permeability for metabolites and artificial compound from the apical side, where nutrients and oxygen would be provided. In order to elucidate additional effects and give an explanation for the observed increased permeability in the BBB, we performed a quantitative MS analysis of untreated cells, cells treated with propofol in its vehicle and cells treated with the vehicle only. The experiments provided evidence that propofol

treatment leads to changes in the proteome of human endothelial brain cells, particularly of pathways involved in metabolic stress, ROS metabolism and DNA damage response (DDR) and recognition.

H2AX is a histone protein from the H2A family, which is activated by phosphorylation. It modulates nucleosome-formation, chromatin-remodeling and is involved in DNA repair. It is a marker for double-strand breaks in dsDNA and it interacts with several other proteins which are involved in DNA repair, such as BRCA1 or MDC1. It has been demonstrated that H2AX plays a role in the transcription of genes regulated by FoxO3a, which is associated with aging/longevity and genomic instability [45]. Therefore, it is possible that down-regulation of H2AX by treatment with propofol has longer lasting effects, which we have been observed in the decreased function of the blood-brain-barrier.

Ferritin has been identified as an iron transporter of the blood-brain-barrier [46]. Upregulation of FTH1 via propofol treatment could therefore increase the iron concentration in the brain, and it has been demonstrated that aging goes along with increased iron concentrations in the brain. In addition, the accumulation of iron in neurons induces damage by apoptosis [47]. The up-regulation of FTH1 observed in our experiments could lead to toxic iron concentrations in the brain, what could explain at least some of the long-lasting side effects of propofol.

Based on the MS results, we could also conclude that the affection of the BBB is most likely an indirect effect, because no cell adhesion molecules have been found among the significantly up-/down-regulated proteins in MS analysis. This means that presence of cell adhesion molecules, which are responsible for the function of the BBB, is not changed among the proteins which were detected. Since we analyzed the function after relatively short time periods (hours), we could only see changes in the given time window and this may explain that we could not observe a direct effect on proteins which are responsible in building the BBB. The observed changes in protein levels have most likely long-lasting effects and could have dramatic side effects for patients. Further investigation is necessary to clarify if maybe the intracellular localization of cell adhesion molecules is affected instead of changes in protein levels. For instance, we cannot exclude changes in posttranslational modifications (PTMs), and it has been reported that a change in PTMs can affect the BBB substantially [48]. That does not only include commonly seen PTMs such as phosphorylation [49] or ubiquitination [50], but also for instance palmitoylation [51]. Since we could see a decrease in H2AX levels upon propofol treatment, it would be interesting to analyze the phosphorylation status of this protein. Since we did not enrich for particular PTMs, such as phosphorylation, we would like to investigate these questions in a potential follow-up study. In addition, ROS can also lead to a direct damage of molecules responsible for forming tight barriers, which underpins the current findings [52]. Furthermore, we could show in a previous study that glycation as it is observed during a severe diabetes mellitus leads in combination with the treatment of propofol to an additive effect regarding an increased permeability of the BBB [22]. In line with this observation, it is likely that other proteins which were detected to be changed after treatment with the vehicle or propofol plus the vehicle are affected by PTMs. For instance, we noticed a slight change of FTH1 towards a higher molecular weight upon treatment with the compounds. This is consistent with previous observations reporting phosphorylation on at least two serine residues of FTH1 [53,54], and could indicate increased phosphorylation in addition to an upregulation of the protein.

We expected to see the level of proteins changed, which are directly involved with building the BBB, for instance occludins, claudins and ZO-proteins. Interestingly, proteins directly involved in building the BBB were shown to be enriched in our pathway analysis. There are several possibilities as to why we do not see a direct effect. Firstly, the effects may take more than a day to show substantial and detectable changes in their levels and will likely not reflect all changes of a complex proteome. Secondly, the effects on the BBB could be dependent on changes of the PTMs. There is evidence that PTMs can modulate the barrier functions in epithelial cell in general and epithelial cells building

the BBB in particular. It has been shown that not only claudins are modified for instance by phosphorylation, palmitoylation ubiquitination and SUMOylation, but also occludins, tricellulins and angulins [55].

In addition, the performed experiments give strong indications that not only propofol can affect the BBB, but also the lipidous vehicle may be able to affect the permeability of the BBB. Propofol is an anesthetic with favorable properties, however, the formulation with lipidous vehicles such as soybean oils has some disadvantages, including emulsion instability, injection pain, a need for antimicrobial agents to prevent sepsis and potential hyperlipidemia-related side effects [33]. Here, we could clearly distinguish in the proteomic profile between the effects of propofol and the respective vehicle. It also underpins the need to develop different, more favorable vehicles with less side effects.

It is obvious that metabolic stress, ROS metabolism and DDR are interconnected, and it may give an explanation for certain observed long-term actions of propofol such as impairment of cognitive function, associated with neuroapoptosis [56,57]. It may well be that an increase of metabolic stress and ROS contribute to apoptosis not only in endothelial cells of the BBB, but also in neurons. In addition, it has been shown that propofol also inhibits long-term potentiation in a rat model, suggesting it has a strong effect on the nervous system potentially via the BBB. Given the potential effect of ROS-species leading to a collapsed BBB, treatment with compounds reducing oxidative stress during and after treatment with propofol may be beneficial. This hypothesis supports our previous observation that a less tighter BBB upon glycation may be partially reduced upon treatment with ascorbic acid, colloquially known as vitamin C [22].

5. Conclusions

Propofol treatment leads to an increased permeability of the BBB. This is accompanied by changes of subproteomic networks associated with metabolic stress and proteins involved in ROS metabolisms as well as DDR. These results may explain some of the long-term effects of propofol on the central nervous system and underpins the benefit of compounds acting as scavengers such as ascorbic acid.

Supplementary Materials: The following are available online at https://www.mdpi.com/article/10.3390/proteomes10030028/s1, Figure S1: PCA plot, Table S1: Differentially_quantified_proteins, Table S2: Peptides, Table S3: Protein, Table S4: PSM.

Author Contributions: Conceptualization, R.H. and H.O.; methodology, M.F. and V.W.; software, M.F.; validation, T.L., K.B. and V.W.; formal analysis, T.L.; investigation, T.L. and V.W.; resources, R.H., B.H., M.F. and H.O.; data curation, T.L. and M.F.; writing—original draft preparation, T.L., R.H. and H.O.; writing—review and editing, R.H., M.F. and H.O.; visualization, T.L. and M.F.; supervision, R.H. and H.O.; project administration, R.H. and H.O.; funding acquisition R.H. and H.O. All authors have read and agreed to the published version of the manuscript.

Funding: This research was funded by the German Research Foundation (DFG GRK 2155 ProMoAge) and internal grants of the Medical Faculty of the Martin-Luther-University (HaPKoM). We acknowledge the financial support within the funding programme Open Access Publishing by the German Research Foundation (DFG).

Institutional Review Board Statement: Not applicable.

Informed Consent Statement: Not applicable.

Data Availability Statement: The mass spectrometry proteomics data have been deposited to the ProteomeXchange Consortium via the PRIDE [44] partner repository with the dataset identifier PXD033856 and 10.6019/PXD033856.

Acknowledgments: The authors acknowledge Annett Thate for technical assistance.

Conflicts of Interest: The authors declare no conflict of interest.

References

1. Montagne, A.; Zhao, Z.; Zlokovic, B.V. Alzheimer's disease: A matter of blood-brain barrier dysfunction? *J. Exp. Med.* **2017**, *214*, 3151–3169. [CrossRef] [PubMed]
2. Ballabh, P.; Braun, A.; Nedergaard, M. The blood-brain barrier: An overview: Structure, regulation, and clinical implications. *Neurobiol. Dis.* **2004**, *16*, 1–13. [CrossRef] [PubMed]
3. Brightman, M.W.; Reese, T.S. Junctions between intimately apposed cell membranes in the vertebrate brain. *J. Cell Biol.* **1969**, *40*, 648–677. [CrossRef] [PubMed]
4. Morris, A.W.; Sharp, M.M.; Albargothy, N.J.; Fernandes, R.; Hawkes, C.A.; Verma, A.; Weller, R.O.; Carare, R.O. Vascular basement membranes as pathways for the passage of fluid into and out of the brain. *Acta Neuropathol.* **2016**, *131*, 725–736. [CrossRef]
5. Coomber, B.L.; Stewart, P.A. Morphometric analysis of CNS microvascular endothelium. *Microvasc. Res.* **1985**, *30*, 99–115. [CrossRef]
6. Betz, A.L.; Goldstein, G.W. Polarity of the blood-brain barrier: Neutral amino acid transport into isolated brain capillaries. *Science* **1978**, *202*, 225–227. [CrossRef]
7. Betz, A.L.; Firth, J.A.; Goldstein, G.W. Polarity of the blood-brain barrier: Distribution of enzymes between the luminal and antiluminal membranes of brain capillary endothelial cells. *Brain Res.* **1980**, *192*, 17–28. [CrossRef]
8. Mittapalli, R.K.; Manda, V.K.; Adkins, C.E.; Geldenhuys, W.J.; Lockman, P.R. Exploiting nutrient transporters at the blood-brain barrier to improve brain distribution of small molecules. *Ther. Deliv.* **2010**, *1*, 775–784. [CrossRef]
9. Oldendorf, W.H.; Cornford, M.E.; Brown, W.J. The large apparent work capability of the blood-brain barrier: A study of the mitochondrial content of capillary endothelial cells in brain and other tissues of the rat. *Ann. Neurol.* **1977**, *1*, 409–417. [CrossRef]
10. Roos, D.H.; Puntel, R.L.; Santos, M.M.; Souza, D.O.; Farina, M.; Nogueira, C.W.; Aschner, M.; Burger, M.E.; Barbosa, N.B.; Rocha, J.B. Guanosine and synthetic organoselenium compounds modulate methylmercury-induced oxidative stress in rat brain cortical slices: Involvement of oxidative stress and glutamatergic system. *Toxicol Vitr.* **2009**, *23*, 302–307. [CrossRef]
11. Palmer, A.M. The role of the blood-CNS barrier in CNS disorders and their treatment. *Neurobiol. Dis.* **2010**, *37*, 3–12. [CrossRef] [PubMed]
12. Evans, M.C.; Couch, Y.; Sibson, N.; Turner, M.R. Inflammation and neurovascular changes in amyotrophic lateral sclerosis. *Mol. Cell Neurosci.* **2013**, *53*, 34–41. [CrossRef] [PubMed]
13. Jeppsson, B.; Freund, H.R.; Gimmon, Z.; James, J.H.; von Meyenfeldt, M.F.; Fischer, J.E. Blood-brain barrier derangement in sepsis: Cause of septic encephalopathy? *Am. J. Surg.* **1981**, *141*, 136–142. [CrossRef]
14. Tighe, D.; Moss, R.; Bennett, D. Cell surface adrenergic receptor stimulation modifies the endothelial response to SIRS. Systemic Inflammatory Response Syndrome. *New Horiz.* **1996**, *4*, 426–442. [PubMed]
15. Pluta, R. Pathological opening of the blood-brain barrier to horseradish peroxidase and amyloid precursor protein following ischemia-reperfusion brain injury. *Chemotherapy* **2005**, *51*, 223–226. [CrossRef] [PubMed]
16. Pluta, R.; Lossinsky, A.S.; Wisniewski, H.M.; Mossakowski, M.J. Early blood-brain barrier changes in the rat following transient complete cerebral ischemia induced by cardiac arrest. *Brain Res.* **1994**, *633*, 41–52. [CrossRef]
17. Zador, Z.; Stiver, S.; Wang, V.; Manley, G.T. Role of aquaporin-4 in cerebral edema and stroke. *Handb. Exp. Pharmacol.* **2009**, *190*, 159–170. [CrossRef]
18. Kim, K.S.; Wass, C.A.; Cross, A.S. Blood-brain barrier permeability during the development of experimental bacterial meningitis in the rat. *Exp. Neurol.* **1997**, *145*, 253–257. [CrossRef]
19. Arshi, A.; Lai, W.C.; Chen, J.B.; Bukata, S.V.; Stavrakis, A.I.; Zeegen, E.N. Predictors and Sequelae of Postoperative Delirium in Geriatric Hip Fracture Patients. *Geriatr. Orthop. Surg. Rehabil.* **2018**, *9*, 2151459318814823. [CrossRef]
20. Young, G.B.; Bolton, C.F.; Archibald, Y.M.; Austin, T.W.; Wells, G.A. The electroencephalogram in sepsis-associated encephalopathy. *J. Clin. Neurophysiol.* **1992**, *9*, 145–152. [CrossRef]
21. Clawson, C.C.; Hartmann, J.F.; Vernier, R.L. Electron microscopy of the effect of gram-negative endotoxin on the blood-brain barrier. *J. Comp. Neurol.* **1966**, *127*, 183–198. [CrossRef]
22. Weber, V.; Olzscha, H.; Langrich, T.; Hartmann, C.; Jung, M.; Hofmann, B.; Horstkorte, R.; Bork, K. Glycation Increases the Risk of Microbial Traversal through an Endothelial Model of the Human Blood-Brain Barrier after Use of Anesthetics. *J. Clin. Med.* **2020**, *9*, 3672. [CrossRef]
23. James, R.; Glen, J.B. Synthesis, biological evaluation, and preliminary structure-activity considerations of a series of alkylphenols as intravenous anesthetic agents. *J. Med. Chem.* **1980**, *23*, 1350–1357. [CrossRef] [PubMed]
24. Chidambaran, V.; Costandi, A.; D'Mello, A. Propofol: A review of its role in pediatric anesthesia and sedation. *CNS Drugs* **2015**, *29*, 543–563. [CrossRef] [PubMed]
25. Wessen, A.; Persson, P.M.; Nilsson, A.; Hartvig, P. Concentration-effect relationships of propofol after total intravenous anesthesia. *Anesth. Analg.* **1993**, *77*, 1000–1007. [PubMed]
26. Shafer, S.L. Advances in propofol pharmacokinetics and pharmacodynamics. *J. Clin. Anesth.* **1993**, *5*, 14–21. [CrossRef]
27. Takizawa, E.; Hiraoka, H.; Takizawa, D.; Goto, F. Changes in the effect of propofol in response to altered plasma protein binding during normothermic cardiopulmonary bypass. *Br. J. Anaesth.* **2006**, *96*, 179–185. [CrossRef] [PubMed]
28. Angelini, G.; Ketzler, J.T.; Coursin, D.B. Use of propofol and other nonbenzodiazepine sedatives in the intensive care unit. *Crit. Care Clin.* **2001**, *17*, 863–880. [CrossRef]

29. Langley, M.S.; Heel, R.C. Propofol. A review of its pharmacodynamic and pharmacokinetic properties and use as an intravenous anaesthetic. *Drugs* **1988**, *35*, 334–372. [CrossRef] [PubMed]
30. Stewart, L.; Bullock, R.; Rafferty, C.; Fitch, W.; Teasdale, G.M. Propofol sedation in severe head injury fails to control high ICP, but reduces brain metabolism. *Acta Neurochir. Suppl. (Wien)* **1994**, *60*, 544–546. [CrossRef]
31. Plunkett, J.J.; Reeves, J.D.; Ngo, L.; Bellows, W.; Shafer, S.L.; Roach, G.; Howse, J.; Herskowitz, A.; Mangano, D.T. Urine and plasma catecholamine and cortisol concentrations after myocardial revascularization. Modulation by continuous sedation. Multicenter Study of Perioperative Ischemia (McSPI) Research Group, and the Ischemia Research and Education Foundation (IREF). *Anesthesiology* **1997**, *86*, 785–796. [CrossRef] [PubMed]
32. Kelbel, I.; Weiss, M. Anaesthetics and immune function. *Curr. Opin. Anaesthesiol.* **2001**, *14*, 685–691. [CrossRef] [PubMed]
33. Baker, M.T.; Naguib, M. Propofol: The challenges of formulation. *Anesthesiology* **2005**, *103*, 860–876. [CrossRef] [PubMed]
34. Li, Y.; Zhong, D.; Lei, L.; Jia, Y.; Zhou, H.; Yang, B. Propofol Prevents Renal Ischemia-Reperfusion Injury via Inhibiting the Oxidative Stress Pathways. *Cell Physiol. Biochem.* **2015**, *37*, 14–26. [CrossRef]
35. Jovic, M.; Stancic, A.; Nenadic, D.; Cekic, O.; Nezic, D.; Milojevic, P.; Micovic, S.; Buzadzic, B.; Korac, A.; Otasevic, V.; et al. Mitochondrial molecular basis of sevoflurane and propofol cardioprotection in patients undergoing aortic valve replacement with cardiopulmonary bypass. *Cell Physiol. Biochem.* **2012**, *29*, 131–142. [CrossRef] [PubMed]
36. Corcoran, T.B.; Engel, A.; Sakamoto, H.; O'Shea, A.; O'Callaghan-Enright, S.; Shorten, G.D. The effects of propofol on neutrophil function, lipid peroxidation and inflammatory response during elective coronary artery bypass grafting in patients with impaired ventricular function. *Br. J. Anaesth.* **2006**, *97*, 825–831. [CrossRef]
37. Fischer, S.; Renz, D.; Kleinstuck, J.; Schaper, W.; Karliczek, G.F. In vitro effects of anaesthetic agents on the blood-brain barrier. *Anaesthesist* **2004**, *53*, 1177–1184. [CrossRef] [PubMed]
38. Zhou, D.; Zhuang, J.; Wang, Y.; Zhao, D.; Zhao, L.; Zhu, S.; Pu, J.; Yin, M.; Zhang, H.; Wang, Z.; et al. Propofol Alleviates DNA Damage Induced by Oxygen Glucose Deprivation and Reperfusion via FoxO1 Nuclear Translocation in H9c2 Cells. *Front. Physiol.* **2019**, *10*, 223. [CrossRef]
39. Weber, V.; Bork, K.; Horstkorte, R.; Olzscha, H. Analyzing the Permeability of the Blood-Brain Barrier by Microbial Traversal through Microvascular Endothelial Cells. *J. Vis. Exp.* **2020**, *14*, e60692. [CrossRef]
40. Ashburner, M.; Ball, C.A.; Blake, J.A.; Botstein, D.; Butler, H.; Cherry, J.M.; Davis, A.P.; Dolinski, K.; Dwight, S.S.; Eppig, J.T.; et al. Gene ontology: Tool for the unification of biology. The Gene Ontology Consortium. *Nat. Genet.* **2000**, *25*, 25–29. [CrossRef] [PubMed]
41. The Gene Ontology Consortium. The Gene Ontology resource: Enriching a GOld mine. *Nucleic Acids Res.* **2021**, *49*, D325–D334. [CrossRef] [PubMed]
42. Stins, M.F.; Badger, J.; Sik Kim, K. Bacterial invasion and transcytosis in transfected human brain microvascular endothelial cells. *Microb. Pathog.* **2001**, *30*, 19–28. [CrossRef] [PubMed]
43. Dagley, L.F.; Infusini, G.; Larsen, R.H.; Sandow, J.J.; Webb, A.I. Universal Solid-Phase Protein Preparation (USP(3)) for Bottom-up and Top-down Proteomics. *J. Proteome Res.* **2019**, *18*, 2915–2924. [CrossRef] [PubMed]
44. Perez-Riverol, Y.; Bai, J.; Bandla, C.; Garcia-Seisdedos, D.; Hewapathirana, S.; Kamatchinathan, S.; Kundu, D.J.; Prakash, A.; Frericks-Zipper, A.; Eisenacher, M.; et al. The PRIDE database resources in 2022: A hub for mass spectrometry-based proteomics evidences. *Nucleic Acids Res.* **2022**, *50*, D543–D552. [CrossRef] [PubMed]
45. Tarrade, S.; Bhardwaj, T.; Flegal, M.; Bertrand, L.; Velegzhaninov, I.; Moskalev, A.; Klokov, D. Histone H2AX Is Involved in FoxO3a-Mediated Transcriptional Responses to Ionizing Radiation to Maintain Genome Stability. *Int. J. Mol. Sci.* **2015**, *16*, 29996–30014. [CrossRef]
46. Fishman, J.B.; Rubin, J.B.; Handrahan, J.V.; Connor, J.R.; Fine, R.E. Receptor-mediated transcytosis of transferrin across the blood-brain barrier. *J. Neurosci. Res.* **1987**, *18*, 299–304. [CrossRef] [PubMed]
47. Killilea, D.W.; Wong, S.L.; Cahaya, H.S.; Atamna, H.; Ames, B.N. Iron accumulation during cellular senescence. *Ann. N. Y. Acad Sci.* **2004**, *1019*, 365–367. [CrossRef] [PubMed]
48. Reiche, J.; Huber, O. Post-translational modifications of tight junction transmembrane proteins and their direct effect on barrier function. *Biochim. Biophys. Acta Biomembr.* **2020**, *1862*, 183330. [CrossRef] [PubMed]
49. Shiomi, R.; Shigetomi, K.; Inai, T.; Sakai, M.; Ikenouchi, J. CaMKII regulates the strength of the epithelial barrier. *Sci. Rep.* **2015**, *5*, 13262. [CrossRef] [PubMed]
50. Marunaka, K.; Furukawa, C.; Fujii, N.; Kimura, T.; Furuta, T.; Matsunaga, T.; Endo, S.; Hasegawa, H.; Anzai, N.; Yamazaki, Y.; et al. The RING finger- and PDZ domain-containing protein PDZRN3 controls localization of the Mg(2+) regulator claudin-16 in renal tube epithelial cells. *J. Biol. Chem.* **2017**, *292*, 13034–13044. [CrossRef]
51. Heiler, S.; Mu, W.; Zoller, M.; Thuma, F. The importance of claudin-7 palmitoylation on membrane subdomain localization and metastasis-promoting activities. *Cell Commun. Signal* **2015**, *13*, 29. [CrossRef]
52. Molina-Jijon, E.; Rodriguez-Munoz, R.; Namorado Mdel, C.; Pedraza-Chaverri, J.; Reyes, J.L. Oxidative stress induces claudin-2 nitration in experimental type 1 diabetic nephropathy. *Free Radic. Biol. Med.* **2014**, *72*, 162–175. [CrossRef]
53. Han, G.; Ye, M.; Zhou, H.; Jiang, X.; Feng, S.; Jiang, X.; Tian, R.; Wan, D.; Zou, H.; Gu, J. Large-scale phosphoproteome analysis of human liver tissue by enrichment and fractionation of phosphopeptides with strong anion exchange chromatography. *Proteomics* **2008**, *8*, 1346–1361. [CrossRef]

54. Olsen, J.V.; Vermeulen, M.; Santamaria, A.; Kumar, C.; Miller, M.L.; Jensen, L.J.; Gnad, F.; Cox, J.; Jensen, T.S.; Nigg, E.A.; et al. Quantitative phosphoproteomics reveals widespread full phosphorylation site occupancy during mitosis. *Sci. Signal* **2010**, *3*, ra3. [CrossRef]
55. Shigetomi, K.; Ikenouchi, J. Regulation of the epithelial barrier by post-translational modifications of tight junction membrane proteins. *J. Biochem.* **2018**, *163*, 265–272. [CrossRef]
56. Han, D.; Jin, J.; Fang, H.; Xu, G. Long-term action of propofol on cognitive function and hippocampal neuroapoptosis in neonatal rats. *Int. J. Clin. Exp. Med.* **2015**, *8*, 10696–10704.
57. Kim, J.L.; Bulthuis, N.E.; Cameron, H.A. The Effects of Anesthesia on Adult Hippocampal Neurogenesis. *Front. Neurosci.* **2020**, *14*, 588356. [CrossRef] [PubMed]

Erklärungen

(1) Ich erkläre, dass ich mich an keiner anderen Hochschule einem Promotionsverfahren unterzogen bzw. eine Promotion begonnen habe.

(2) Ich erkläre, die Angaben wahrheitsgemäß gemacht und die wissenschaftliche Arbeit an keiner anderen wissenschaftlichen Einrichtung zur Erlangung eines akademischen Grades eingereicht zu haben.

(3) Ich erkläre an Eides statt, dass ich die Arbeit selbstständig und ohne fremde Hilfe verfasst habe. Alle Regeln der guten wissenschaftlichen Praxis wurden eingehalten; es wurden keine anderen als die von mir angegebenen Quellen und Hilfsmittel benutzt und die den benutzten Werken wörtlich oder inhaltlich entnommenen Stellen als solche kenntlich gemacht.

Halle (Saale), den 17.06.2024